

FINITE DEFORMATION PLASTICITY FOR COMPOSITE STRUCTURES:
COMPUTATIONAL MODELS AND ADAPTIVE STRATEGIES

by

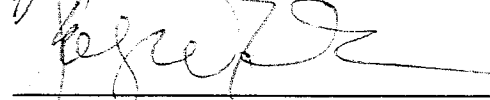
Kamlun Shek

A Thesis Submitted to the Graduate
Faculty of Rensselaer Polytechnic Institute
in Partial Fulfillment of the
Requirements for the Degree of
DOCTOR OF PHILOSOPHY
Major Subject: Mechanical Engineering


Approved by the
Examining Committee:



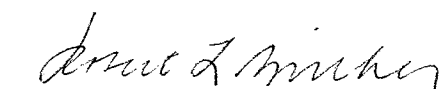
Jacob Fish, Thesis Advisor



George J. Dvorak, Thesis Co-Advisor



Mark S. Shephard, Member



Robert L. Spilker, Member

Rensselaer Polytechnic Institute
Troy, New York

July 1997

(For Graduation August 1997)

Dedicate to my parents

© Copyright 1997

by

Kamlun Shek

All Rights Reserved

ii

CONTENTS

LIST OF FIGURES	v
ACKNOWLEDGEMENT	vi
ABSTRACT.....	vii
1. INTRODUCTION	1
2. MATHEMATICAL HOMOGENIZATION WITH EIGENSTRAIN FOR SMALL DEFORMATIONS	5
2.1 Problem Definition	5
2.2 Asymptotic Analysis	7
2.3 2-Point Scheme for Two Phase Composites	14
3. THE 2-POINT SCHEME FOR FINITE DEFORMATION PLASTICITY	16
3.1 Basic Assumptions	16
3.2 Implicit Integration of Constitutive Equation	20
3.3 Consistent Linearization	23
4. THE n -POINT SCHEME FOR FINITE DEFORMATION PLASTICITY	30
4.1 Governing Equations	30
4.2 Implicit Integration of Constitutive Equations	33
4.3 Consistent Linearization for Incremental Homogenization Scheme	35
5. ADAPTIVE MODEL CONSTRUCTION	40
5.1 Modeling Error Estimation	40
5.2 Adaptive 2/ n -Point Scheme	42
6. NUMERICAL EXPERIMENTS	46
6.1 Uniform Macro-Strain Loading	46
6.2 The 3D Beam Problem	47
6.3 The Nozzle Flap Problem	48
7. CONCLUSIONS AND FUTURE RESEARCH DIRECTIONS	56

REFERENCES57

Appendix A: DERIVATION OF $\partial(\sigma_{ij}^{(m)} - \alpha_{ij}^{(m)})/\partial\Delta\lambda^{(m)}$ 61

Appendix B: LINEARIZATION OF $\Delta\bar{\epsilon}_{ij}$ AND $\Delta\bar{\omega}_{ij}$ 63

LIST OF FIGURES

Figure 1.1	Finite element mesh for the nozzle flap problem	4
Figure 1.2	Finite element mesh for the fibrous unit cell	4
Figure 2.1	Macroscopic and microscopic structures	15
Figure 3.1	Decomposition of deformation in the microstructure	29
Figure 5.1	Adaptive model construction	45
Figure 6.1	Deformation of unit cell under transverse tension	49
Figure 6.2	Deformation of unit cell under transverse shear	49
Figure 6.3	Deformation of unit cell under longitudinal shear	49
Figure 6.4	Finite element mesh for the 3D beam problem	50
Figure 6.5	Distribution of the normalized local error with the 2-point model	51
Figure 6.6	Effective stress and normalized error at point A with the 2-point model	51
Figure 6.7	Distribution of the normalized local error with the $2/n$ -point model	52
Figure 6.8	Effective stress and normalized error at point B with the $2/n$ -point model	52
Figure 6.9	Geometric model and FE mesh of the plain weave unit cell	53
Figure 6.10	Distribution of the normalized local error in the nozzle flap with plain weave unit cell	54
Figure 6.11	Effective stress and normalized error for fibrous unit cell	55
Figure 6.12	Effective stress and normalized error for plain weave unit cell	55

ACKNOWLEDGEMENT

I would like to express my sincere gratitude to my thesis advisor and co-advisor, Professors Jacob Fish and George J. Dvorak. Professor Fish's instructive guidance and creative nature of thought, and the pioneer work on the Transformation Field Analysis by Prof. Dvorak have been most valuable to this work.

I am also grateful to the other members of my dissertation committee, Professors Mark S. Shephard and Robert L. Spilker for their interest and valuable comments. My wife, Joan, and my daughter, Victoria, receive my special thanks for their love and understanding. I am honored to dedicate this thesis to my parents; without their constant love and support this work would not have been possible.

Finally, the financial support for this work from ARPA/ONR Mechanism-Based Design of Composite Structures program at Rensselaer Polytechnic Institute under grant N00014-92-J-1779 and from the Air Force Office of Scientific Research under grant F49620-97-1-0090 is gratefully acknowledged.

ABSTRACT

This thesis generalizes the classical mathematical homogenization theory for heterogeneous medium to account for eigenstrains. Starting from the double scale asymptotic expansion for the displacement and eigenstrain fields, this study derives close form expressions relating arbitrary eigenstrains to the mechanical fields in the phases.

Computational models and adaptive modeling strategies for obtaining an approximate solution to a boundary value problem describing the finite deformation plasticity of heterogeneous structures are developed. A nearly optimal mathematical model consists of an averaging scheme based on approximating eigenstrains and elastic concentration factors in each micro phase by a constant in the macro problem subdomains where modeling errors are small, whereas elsewhere, a more detailed mathematical model based on piecewise constant approximation of eigenstrains and elastic concentration factors is utilized. The methodology is developed within the framework of "statistically homogeneous" composite material and local periodicity assumptions.

For numerical examples considered, the CPU time obtained by means of the adaptive $2/n$ -point scheme was 30 seconds on a SPARC 10/51 station as opposed to 7 hours using classical mathematical homogenization theory. At the same time, the maximum error in the microscope fields in the critical unit cell was only 3.5% in comparison with the classical mathematical homogenization theory.

CHAPTER 1

INTRODUCTION

In this thesis, we develop a theory and methodology for obtaining an approximate solution to a boundary value problem describing the finite deformation plasticity of heterogeneous structures. The theory is developed within the framework of “statistically homogeneous” composite material and local periodicity assumptions. For readers interested in theoretical and computational issues dealing with various aspects of nonperiodic heterogeneous media we refer to [14][16] [38][49].

In modeling heterogeneous media it is tempting to adopt a macroscopic point of view, which considers the composite as a homogeneous medium with anisotropic properties that have to be determined. Several authors [40] applied anisotropic yield criterion developed by Hill [22] for elastoplastic analysis of fibrous composites. On the other hand Dvorak and Rao [12] and Lin et al. [33] have shown that Hill’s anisotropic yield criterion (originally designed for metals) assuming that hydrostatic stress does not influence yielding and that there is no Bauschinger effect is not valid for fibrous composites.

Under these circumstances micromechanical analysis of composite materials, which provides the overall composite behavior from the properties of individual constituents (reinforcement and matrix) and their interaction, seems to be the only viable alternative. Most of the current micromechanical methods approximate the local fields within each phase either as uniform [1][7][9] or as piecewise constant [2][3][11][46]. Micromechanical approaches can be also classified into the following two categories: (i) those that require evaluation of instantaneous concentration function by solving the rate form of an inclusion or unit cell problem [1][2][3][7][10][46], and (ii) those that require evaluation of elastic concentration function only. The latter is based on the transformation field analysis recently developed by Dvorak [7][8][11]. An excellent survey of these micromechanical approaches for plasticity of fibrous composites is given in [7][9] and references therein provide good insight into this approach.

The challenge of solving structural problems with accurate resolution of microstructural fields undergoing inelastic deformation is enormous. This subject has been an active area of research in the computational mechanics community for more than two decades. Numerous studies have dealt with the utilization of the finite element method [19][20][27][30][31][34][41][46], the boundary element method [18], the Voronoi cell method [17], the spectral method [1], the transformation field analysis [8], and the Fourier series expansion technique [36] for solving PDEs arising from

the homogenization of nonlinear composites. The primary goals of these studies were twofold: (i) develop macroscopic constitutive equations that would enable solution of an auxiliary problem with nonlinear homogenized (smooth) coefficients, and (ii) establish bounds for overall nonlinear properties [3][39][44][45][46][47].

Methods based on a multiple scale asymptotic expansion, which are parallel to micromechanical approaches for linear systems appeared in the mid 70's by the name of mathematical homogenization. The mathematical homogenization method is advantageous in the sense that it provides convergence characteristics of certain norms of interest in addition to the bounds of equivalent material properties. The fundamentals of mathematical homogenization theory can be found, among others, in [4][5][28].

For small deformation plasticity a mathematical homogenization theory has been established by Suquet [44][45]. Finite element application issues were addressed in [19]. In these attempts the uncoupling of scales was carried out for a linearized system in a similar fashion to that of the linear problem. References [2][3][46] represent the micromechanical approaches parallel to the mathematical homogenization for plasticity [19][44][45] in terms of the formulation and computational complexity involved.

Attempts at solving large scale nonlinear structural systems with accurate resolution of microstructural fields are very rare [13][19][28] and successes were reported for small problems and/or special cases. This is because for linear problems a unit cell or a representative volume problem has to be solved only once, whereas for nonlinear history dependent systems, it has to be solved at every increment and for each macroscopic (Gauss) point. Furthermore, history data has to be updated at a number of integration points equal to the product of the number of Gauss points in the macro and micro (unit cell) domains.

To illustrate the computational complexity involved we consider an elasto-plastic analysis of the composite flap problem [15] with fibrous microstructure as shown in Figures 1.1 and 1.2. The structural problem is discretized with 788 tetrahedral elements (993 degrees of freedom), whereas fibrous microstructure is discretized with 98 elements in the fiber domain and 253 elements in the matrix domain, totaling 330 degrees of freedom. The CPU time on SPARC 10/51 workstation for this problem was over 7 hours, as opposed to 10 seconds if von Mises metal plasticity was used instead, which means that 99.9% of CPU time is spent on stress updates. Under these circum-

stances it seems that the statement made by Hill [24] that "... for non-linear systems, the computations needed to establish any constitutive law are formidable indeed ..." is still valid 30 years later.

With the exception of [13][19][28] most of the research activities focused on small deformation inelastic response of microconstituents and their interfaces. This is partially justified due to high stiffness and relatively low ductility of fibrous composite materials. However, when hardening is low and the stress measures are comparable to the inelastic tangent modulus, or in the case of thin structures undergoing large rotations, large deformation formulation is required.

One of the objectives of the present work is to develop a mathematical homogenization theory with eigenstrains, a counterpart to the micromechanical approach based on the transformation field analysis recently developed by Dvorak [6][8]. In Chapter 2 we derive a closed form expression relating arbitrary transformation fields to mechanical fields in the phases, which for the case of piecewise constant transformation fields reduce to the form derived by Dvorak [6] on the basis of the uniform fields concept. The mathematical homogenization theory with eigenstrains is then extended to account for finite deformation and thermal effects in Chapter 3.

The second objective is to devise an efficient computational scheme that will enable to solve large scale structural systems in heterogeneous media. An adaptive strategy is developed to ensure reliability and efficiency of computations. In Chapters 3 and 4 we employ an additive decomposition of the rate of deformation into elastic rate of deformation, governed by hypoelasticity and inelastic rate of deformation. Chapter 3 focuses on the 2-point approximation scheme (for two phase materials), where each point represents an average response within a phase. The local response within each phase is then recovered by means of post-processing. In Chapter 4 we describe the n -point scheme model, where n denotes the number of elements in the microstructure. Chapter 5 is devoted to modeling error estimation and adaptive strategy. We devise an adaptive $2/n$ -point model, where the 2-point scheme is used in regions where modeling errors are small, whereas elsewhere the n -point scheme is employed. Numerical experiments conducted in Chapter 6 investigate the 2-point, the n -point, and the adaptive $2/n$ -point schemes in the context of finite deformation plasticity.

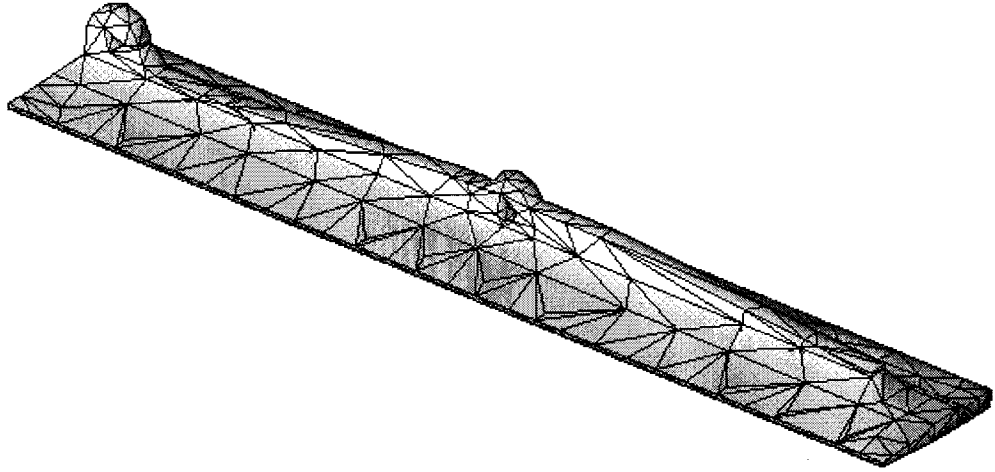


Figure 1.1 Finite element mesh for the nozzle flap problem

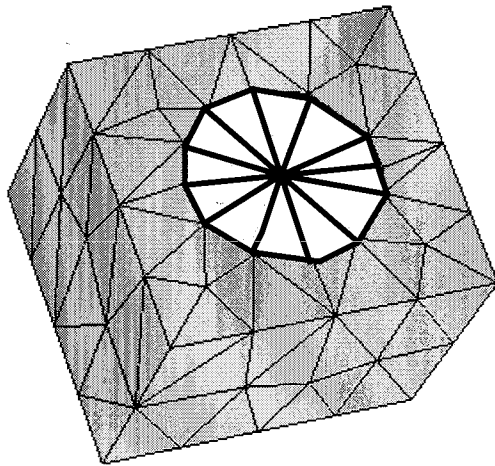


Figure 1.2 Finite element mesh for the fibrous unit cell

CHAPTER 2

MATHEMATICAL HOMOGENIZATION WITH EIGENSTRAIN FOR SMALL DEFORMATIONS

In this section we generalize the classical mathematical homogenization theory [4][5] for heterogeneous media to account for eigenstrains. We regard all inelastic strains, phase transformation and temperature effects as eigenstrains in an otherwise elastic body. We will derive closed form expressions relating arbitrary eigenstrains to mechanical fields in a multi-phase composite medium. In this section attention is restricted to small deformations.

2.1 Problem Definition

The microstructure of a composite material is assumed to be locally periodic (Y-periodic) with a period represented by a unit cell domain or a Representative Volume Element (RVE), denoted by Θ , as shown in Figure 2.1. Y-periodicity implies that all response functions, such as displacements, stresses and strains, are periodic with periods proportional to the ratio of the representative micro and macro structures, denoted by ζ . Let \mathbf{x} be a macroscopic coordinate vector in macro domain Ω and $\mathbf{y} \equiv \mathbf{x}/\zeta$ be a microscopic position vector in Θ . For any periodic function f , we have $f(\mathbf{x}, \mathbf{y}) = f(\mathbf{x}, \mathbf{y} + \mathbf{k}\hat{\mathbf{y}})$ in which vector $\hat{\mathbf{y}}$ is the basic period of the microstructure and \mathbf{k} is a 3 by 3 diagonal matrix with integer components. Adopting the classical nomenclature, any Y-periodic function f can be represented as

$$f^\zeta(\mathbf{x}) \equiv f(\mathbf{x}, \mathbf{y}(\mathbf{x})) \quad (2.1)$$

where superscript ζ denotes a Y-periodic function f . The indirect macroscopic spatial derivatives of f^ζ can be calculated by the chain rule as

$$f_{,x_i}^\zeta(\mathbf{x}) \equiv f_{,x_i}(\mathbf{x}, \mathbf{y}) = f_{,x_i}(\mathbf{x}, \mathbf{y}) + \frac{1}{\zeta} f_{,y_i}(\mathbf{x}, \mathbf{y}) \quad (2.2)$$

$$f_{,y_i}(\mathbf{x}, \mathbf{y}) = f_{,y_i}(\mathbf{x}, \mathbf{y}) + \zeta f_{,x_i}(\mathbf{x}, \mathbf{y}) = \zeta f_{,x_i}(\mathbf{x}, \mathbf{y}) \quad (2.3)$$

where the comma followed by a subscript variable x_i or y_i denotes a partial derivative with respect to the subscript variable (i.e. $f_{,x_i} \equiv \partial f / \partial x_i$ and $f_{,y_i} \equiv \partial f / \partial y_i$). A semi-colon followed

by a subscript variable x_i denotes a partial derivative with respect to the remaining x components (2.2), but a full derivative with respect to y_i , and vice versa when a semi-colon is followed by subscript variable y_i (2.3). Summation convention for repeated right hand side subscripts is employed, except for subscripts x and y .

We assume that micro-constituents possess homogeneous properties and satisfy equilibrium, constitutive, kinematics and compatibility equations as well as jump conditions at the interface between the micro-phases. The corresponding boundary value problem is governed by the following equations:

$$\sigma_{ij;x_j}^\xi + b_i = 0 \quad \text{in } \Omega \quad (2.4)$$

$$\sigma_{ij}^\xi = L_{ijkl}(\varepsilon_{kl}^\xi - \mu_{kl}^\xi) \quad \text{in } \Omega \quad (2.5)$$

$$\varepsilon_{ij}^\xi = u_{(i;x_j)}^\xi \quad \text{in } \Omega \quad (2.6)$$

$$\omega_{ij}^\xi = u_{[i;x_j]}^\xi \quad \text{in } \Omega \quad (2.7)$$

$$u_i^\xi = \bar{u}_i \quad \text{on } \Gamma_u \quad (2.8)$$

$$\sigma_{ij}^\xi n_j = \bar{t}_i \quad \text{on } \Gamma_t \quad (2.9)$$

where σ_{ij}^ξ , ε_{ij}^ξ and ω_{ij}^ξ are components of stress, strain and rotation tensors; L_{ijkl} and μ_{ij}^ξ are components of elastic stiffness and eigenstrain tensors, respectively; b_i is a body force assumed to be independent of \mathbf{y} ; u_i^ξ denotes the components of the displacement vector; the subscript pairs with regular and square parentheses denote the symmetric and anti-symmetric gradients defined as

$$u_{(i;x_j)}^\xi \equiv \frac{1}{2}(u_{i;x_j}^\xi + u_{j;x_i}^\xi) \quad \text{and} \quad u_{[i;x_j]}^\xi \equiv \frac{1}{2}(u_{i;x_j}^\xi - u_{j;x_i}^\xi) \quad (2.10)$$

Ω denotes the macroscopic domain of interest with boundary Γ ; Γ_u and Γ_t are boundary portions where displacements \bar{u}_i and tractions \bar{t}_i are prescribed, respectively, such that

$\Gamma_u \cap \Gamma_t = \emptyset$ and $\Gamma = \Gamma_u \cup \Gamma_t$; n_i denotes the normal vector on Γ . We assume that the interface between the phases is perfectly bonded, i.e. $[\sigma_{ij}^\zeta \hat{n}_j] = 0$ and $[u_i^\zeta] = 0$ at the interface, Γ_{int} , where \hat{n}_i is the normal vector to Γ_{int} and $[\bullet]$ is a jump operator.

2.2 Asymptotic Analysis

In the following, displacements $u_i^\zeta(\mathbf{x}) = u_i(\mathbf{x}, \mathbf{y})$ and eigenstrains $\mu_{ij}^\zeta(\mathbf{x}) = \mu_{ij}(\mathbf{x}, \mathbf{y})$ are approximated in terms of double scale asymptotic expansions on $\Omega \times \Theta$:

$$u_i(\mathbf{x}, \mathbf{y}) \approx u_i^0(\mathbf{x}, \mathbf{y}) + \zeta u_i^1(\mathbf{x}, \mathbf{y}) + \dots \quad (2.11)$$

$$\mu_{ij}(\mathbf{x}, \mathbf{y}) \approx \mu_{ij}^0(\mathbf{x}, \mathbf{y}) + \zeta \mu_{ij}^1(\mathbf{x}, \mathbf{y}) + \dots \quad (2.12)$$

Strain and rotation expansions on $\Omega \times \Theta$ can be obtained by substituting (2.11) into (2.6) and (2.7) with consideration of the indirect differentiation rule (2.2)

$$\varepsilon_{ij}(\mathbf{x}, \mathbf{y}) \approx \frac{1}{\zeta} \varepsilon_{ij}^{-1}(\mathbf{x}, \mathbf{y}) + \varepsilon_{ij}^0(\mathbf{x}, \mathbf{y}) + \zeta \varepsilon_{ij}^1(\mathbf{x}, \mathbf{y}) + \dots \quad (2.13)$$

$$\omega_{ij}(\mathbf{x}, \mathbf{y}) \approx \frac{1}{\zeta} \omega_{ij}^{-1}(\mathbf{x}, \mathbf{y}) + \omega_{ij}^0(\mathbf{x}, \mathbf{y}) + \zeta \omega_{ij}^1(\mathbf{x}, \mathbf{y}) + \dots \quad (2.14)$$

where strain and rotation components for various orders of ζ are given as

$$\varepsilon_{ij}^{-1} = \varepsilon_{yij}(\mathbf{u}^0), \quad \varepsilon_{ij}^s = \varepsilon_{xij}(\mathbf{u}^s) + \varepsilon_{yij}(\mathbf{u}^{s+1}), \quad s = 0, 1, \dots \quad (2.15)$$

$$\omega_{ij}^{-1} = \omega_{yij}(\mathbf{u}^0), \quad \omega_{ij}^s = \omega_{xij}(\mathbf{u}^s) + \omega_{yij}(\mathbf{u}^{s+1}), \quad s = 0, 1, \dots \quad (2.16)$$

and

$$\varepsilon_{xij}(\mathbf{u}^s) = u_{(i,x_j)}^s, \quad \varepsilon_{yij}(\mathbf{u}^s) = u_{(i,y_j)}^s \quad (2.17)$$

$$\omega_{xij}(\mathbf{u}^s) = u_{[i,x_j]}^s, \quad \omega_{yij}(\mathbf{u}^s) = u_{[i,y_j]}^s \quad (2.18)$$

Stresses and strains for different orders of ζ are related by the constitutive equation (2.5)

$$\sigma_{ij}^{-1} = L_{ijkl} \varepsilon_{kl}^{-1}, \quad \sigma_{ij}^s = L_{ijkl} (\varepsilon_{kl}^s - \mu_{kl}^s), \quad s = 0, 1, \dots \quad (2.19)$$

The resulting asymptotic expansion of stress is given as

$$\sigma_{ij}(\mathbf{x}, \mathbf{y}) \approx \frac{1}{\zeta} \sigma_{ij}^{-1}(\mathbf{x}, \mathbf{y}) + \sigma_{ij}^0(\mathbf{x}, \mathbf{y}) + \zeta \sigma_{ij}^1(\mathbf{x}, \mathbf{y}) + \dots \quad (2.20)$$

Inserting the stress expansion (2.20) into equilibrium equation (2.4) and making the use of (2.2) yields the following equilibrium equations for various orders:

$$O(\zeta^{-2}): \quad \sigma_{ij,y_j}^{-1} = 0 \quad (2.21)$$

$$O(\zeta^{-1}): \quad \sigma_{ij,x_j}^{-1} + \sigma_{ij,y_j}^0 = 0 \quad (2.22)$$

$$O(\zeta^0): \quad \sigma_{ij,x_j}^0 + \sigma_{ij,y_j}^1 + b_i = 0 \quad (2.23)$$

$$O(\zeta^s): \quad \sigma_{ij,x_j}^s + \sigma_{ij,y_j}^{s+1} = 0, \quad s = 1, 2, \dots \quad (2.24)$$

Consider the $O(\zeta^{-2})$ equilibrium equation (2.21) first. Pre-multiplying it by u_i^0 and integrating over a unit cell domain Θ yields

$$\int_{\Theta} u_i^0 \sigma_{ij,y_j}^{-1} d\Theta = 0 \quad (2.25)$$

and subsequently integrating by parts gives

$$\int_{\Gamma_{\Theta}} u_i^0 \sigma_{ij}^{-1} n_j d\Gamma_{\Theta} - \int_{\Theta} u_{(i,y_j)}^0 L_{ijkl} u_{(k,y_l)}^0 d\Theta = 0 \quad (2.26)$$

where Γ_{Θ} denotes the boundary of Θ . The boundary integral term in (2.26) vanishes due to the periodicity of boundary conditions on Γ_{Θ} . Furthermore, since the elastic stiffness L_{ijkl} is positive definite, we have

$$u_{(i,y_j)}^0 = 0 \quad \Rightarrow \quad u_i^0 = u_i^0(\mathbf{x}) \quad (2.27)$$

and

$$\sigma_{ij}^{-1}(\mathbf{x}, \mathbf{y}) = \varepsilon_{ij}^{-1}(\mathbf{x}, \mathbf{y}) = \omega_{ij}^{-1}(\mathbf{x}, \mathbf{y}) = 0 \quad (2.28)$$

We proceed to the $O(\zeta^{-1})$ equilibrium equation (2.22) next. From equations (2.15) and (2.19) follows

$$\{L_{ijkl}(\varepsilon_{xkl}(\mathbf{u}^0) + \varepsilon_{ykl}(\mathbf{u}^1) - \mu_{kl}^0)\}_{,y_j} = 0 \quad \text{on} \quad \Theta \quad (2.29)$$

To solve for (2.29) up to a constant we introduce the following separation of variables

$$u_i^1(\mathbf{x}, \mathbf{y}) = H_{ikl}(\mathbf{y})\{\varepsilon_{xkl}(\mathbf{u}^0) + d_{kl}^\mu(\mathbf{x})\} \quad (2.30)$$

where H_{ikl} is a Y -periodic function, d_{kl}^μ is a macroscopic portion of the solution resulting from eigenstrains, i.e. if $\mu_{kl}^0(\mathbf{x}, \mathbf{y}) = 0$ then $d_{kl}^\mu(\mathbf{x}) = 0$. It should be noted that both H_{ikl} and d_{kl}^μ are symmetric with respect to indices k and l . Based on (2.30) $O(\zeta^{-1})$ equilibrium equation takes the following form:

$$\{L_{ijkl}((I_{klmn} + G_{klmn})\varepsilon_{xmn}(\mathbf{u}^0) + G_{klmn}d_{mn}^\mu(\mathbf{x}) - \mu_{kl}^0)\}_{,y_j} = 0 \quad \text{on} \quad \Theta \quad (2.31)$$

where

$$I_{klmn} = \frac{1}{2}(\delta_{mk}\delta_{nl} + \delta_{nk}\delta_{ml}), \quad G_{klmn}(\mathbf{y}) = H_{(k,y_l)mn}(\mathbf{y}) \quad (2.32)$$

and δ_{mk} is the Kronecker delta. Since equation (2.31) should be valid for arbitrary combination of macroscopic strain field $\varepsilon_{xmn}(\mathbf{u}^0)$ and eigenstrain field μ_{kl}^0 , we first consider $\mu_{kl}^0 \equiv 0$, $\varepsilon_{xmn}(\mathbf{u}^0) \neq 0$ and then $\varepsilon_{xmn}(\mathbf{u}^0) \equiv 0$, $\mu_{kl}^0 \neq 0$ which yields the following two governing equations on Θ :

$$\{L_{ijkl}(I_{klmn} + H_{(k,y_l)mn})\}_{,y_j} = 0 \quad (2.33)$$

$$\{L_{ijkl}(H_{(k,y_l)mn}d_{mn}^\mu(\mathbf{x}) - \mu_{kl}^0)\}_{,y_j} = 0 \quad (2.34)$$

Equation (2.33) together with the periodic boundary conditions comprise a standard linear boundary value problem on Θ . For complex microstructures the finite element method is often used to discretize the system to solve for $H_{ikl}(\mathbf{y})$, which yields a set of linear algebraic system with six

right hand side vectors [14][19]. In absence of eigenstrains, the asymptotic fields can be written in terms of the macroscopic strain $\bar{\varepsilon}_{ij} \equiv \varepsilon_{xij}(\mathbf{u}^0)$ and the macroscopic rotation $\bar{\omega}_{ij} \equiv \omega_{xij}(\mathbf{u}^0)$:

$$\varepsilon_{ij} = \bar{\varepsilon}_{ij} + G_{ijkl}\bar{\varepsilon}_{kl} + O(\zeta) \quad (2.35)$$

$$\omega_{ij} = \bar{\omega}_{ij} + \hat{G}_{ijkl}\bar{\varepsilon}_{kl} + O(\zeta) \quad (2.36)$$

where

$$\hat{G}_{ijkl}(\mathbf{y}) = H_{[i,y]kl}(\mathbf{y}) \quad (2.37)$$

The terms G_{ijkl} and \hat{G}_{ijkl} are known as polarization functions. It can be shown that the integrals of the polarization functions on Θ vanish due to periodicity conditions.

The elastic homogenized stiffness \bar{L}_{ijkl} follows from $O(\zeta^0)$ equilibrium equation [14]:

$$\bar{L}_{ijkl} \equiv \frac{1}{|\Theta|} \int_{\Theta} L_{ijmn} A_{mnkl} d\Theta = \frac{1}{|\Theta|} \int_{\Theta} A_{mnij} L_{mnst} A_{stkl} d\Theta \quad (2.38)$$

where

$$A_{klmn} = I_{klmn} + G_{klmn} \quad (2.39)$$

A_{klmn} is often referred to as an elastic strain concentration function and $|\Theta|$ is the volume of a unit cell.

After solving (2.33) for H_{imn} , we proceed to (2.34) for finding d_{kl}^{μ} subjected to periodic boundary conditions. Pre-multiplying (2.34) by H_{ist} and then integrating the resulting equation by parts with consideration of the periodic boundary conditions yields

$$\int_{\Theta} G_{ijst} L_{ijkl} (G_{klmn} d_{mn}^{\mu}(\mathbf{x}) - \mu_{kl}^0) d\Theta = 0 \quad (2.40)$$

Rewriting this equation in terms of strain concentration function A_{ijkl} and manipulating it with (2.38) yields

$$d_{ij}^{\mu} = \frac{1}{|\Theta|} (\tilde{L}_{ijkl} - \bar{L}_{ijkl})^{-1} \int_{\Theta} G_{mnkl} L_{mnst} \mu_{st}^0 d\Theta \quad (2.41)$$

where

$$\tilde{L}_{ijkl} = \frac{1}{|\Theta|} \int_{\Theta} L_{ijkl} d\Theta \quad (2.42)$$

The superscript -1 denotes the reciprocal tensor. The $O(\zeta^0)$ approximation to the asymptotic strain (2.13) and rotation fields (2.14) reduces to:

$$\varepsilon_{ij} = \bar{\varepsilon}_{ij} + G_{ijkl}(\bar{\varepsilon}_{kl} + d_{kl}^{\mu}) + O(\zeta) \quad (2.43)$$

$$\omega_{ij} = \bar{\omega}_{ij} + \hat{G}_{ijkl}(\bar{\varepsilon}_{kl} + d_{kl}^{\mu}) + O(\zeta) \quad (2.44)$$

Let $\Psi \equiv \{\psi^{(\eta)}(\mathbf{y})\}_1^n$ be a set of C^{-1} continuous functions, then the separation of variables for the $O(\zeta^0)$ eigenstrains is assumed to have the following decomposition:

$$\mu_{ij}^0(\mathbf{x}, \mathbf{y}) = \sum_{\eta=1}^n \psi^{(\eta)}(\mathbf{y}) \mu_{ij}^{(\eta)}(\mathbf{x}) \quad (2.45)$$

The resulting asymptotic expansion of the strain and rotation fields (2.13), (2.14) can be expressed as follows:

$$\varepsilon_{ij}(\mathbf{x}, \mathbf{y}) = \bar{\varepsilon}_{ij}(\mathbf{x}) + G_{ijkl}(\mathbf{y}) \bar{\varepsilon}_{kl}(\mathbf{x}) + \sum_{\eta=1}^n D_{ijkl}^{(\eta)}(\mathbf{y}) \mu_{kl}^{(\eta)}(\mathbf{x}) + O(\zeta) \quad (2.46)$$

$$\omega_{ij}(\mathbf{x}, \mathbf{y}) = \bar{\omega}_{ij}(\mathbf{x}) + \hat{G}_{ijkl}(\mathbf{y}) \bar{\varepsilon}_{kl}(\mathbf{x}) + \sum_{\eta=1}^n \hat{D}_{ijkl}^{(\eta)}(\mathbf{y}) \mu_{kl}^{(\eta)}(\mathbf{x}) + O(\zeta) \quad (2.47)$$

where $D_{ijkl}^{(\eta)}(\mathbf{y})$ and $\hat{D}_{ijkl}^{(\eta)}(\mathbf{y})$ are the eigenstrain influence functions, which can be expressed in terms of polarization functions $G_{ijkl}(\mathbf{y})$ and $\hat{G}_{ijkl}(\mathbf{y})$ as follows

$$D_{ijkl}^{(\eta)}(\mathbf{y}) = \frac{1}{|\Theta|} G_{ijmn} (\tilde{L}_{mnpq} - \bar{L}_{mnpq})^{-1} \int_{\Theta} G_{rspq} L_{rskl} \Psi^{(\eta)} d\Theta \quad (2.48)$$

$$\hat{D}_{ijkl}^{(\eta)}(\mathbf{y}) = \frac{1}{|\Theta|} \hat{G}_{ijmn} (\tilde{L}_{mnpq} - \bar{L}_{mnpq})^{-1} \int_{\Theta} G_{rspq} L_{rskl} \Psi^{(\eta)} d\Theta \quad (2.49)$$

In particular, if Ψ is a set of piecewise constant functions such that

$$\Psi^{(\eta)}(\mathbf{y}_\rho) = \begin{cases} 1 & \text{if } \mathbf{y}_\rho \in \Theta^{(\eta)} \\ 0 & \text{otherwise} \end{cases} \quad (2.50)$$

and $\Theta^{(\eta)}$ is the subdomain η within a unit cell, $c^{(\eta)}$ the subdomain volume fraction given by $c^{(\eta)} \equiv |\Theta^{(\eta)}|/|\Theta|$ and satisfying $\sum_{\eta=1}^n c^{(\eta)} = 1$, then (2.46) and (2.47) reduce to:

$$\varepsilon_{ij}^{(\rho)} = \frac{1}{|\Theta^{(\rho)}|} \int_{\Theta^{(\rho)}} \varepsilon_{ij} d\Theta = \bar{\varepsilon}_{ij} + G_{ijkl}^{(\rho)} \bar{\varepsilon}_{kl} + \sum_{\eta=1}^n D_{ijkl}^{(\rho\eta)} \mu_{kl}^{(\eta)} + O(\zeta) \quad (2.51)$$

$$\omega_{ij}^{(\rho)} = \frac{1}{|\Theta^{(\rho)}|} \int_{\Theta^{(\rho)}} \omega_{ij} d\Theta = \bar{\omega}_{ij} + \hat{G}_{ijkl}^{(\rho)} \bar{\varepsilon}_{kl} + \sum_{\eta=1}^n \hat{D}_{ijkl}^{(\rho\eta)} \mu_{kl}^{(\eta)} + O(\zeta) \quad (2.52)$$

where

$$D_{ijkl}^{(\rho\eta)} = c^{(\eta)} G_{ijmn}^{(\rho)} (\tilde{L}_{mnpq} - \bar{L}_{mnpq})^{-1} G_{rspq}^{(\eta)} L_{rskl}^{(\eta)} \quad (2.53)$$

$$\hat{D}_{ijkl}^{(\rho\eta)} = c^{(\eta)} \hat{G}_{ijmn}^{(\rho)} (\tilde{L}_{mnpq} - \bar{L}_{mnpq})^{-1} G_{rspq}^{(\eta)} L_{rskl}^{(\eta)} \quad (2.54)$$

and

$$(G_{ijkl}^{(\eta)}, \hat{G}_{ijkl}^{(\eta)}) = \frac{1}{|\Theta^{(\eta)}|} \int_{\Theta^{(\eta)}} (G_{ijkl}, \hat{G}_{ijkl}) d\Theta \quad (2.55)$$

We will refer to the piecewise constant model defined by (2.51) and (2.52) as the n -point scheme model. Equation (2.51) has been originally derived by Dvorak [7][8] on the basis of transformation field analysis. Finally, we integrate the $O(\zeta^0)$ equilibrium equation (2.23) over Θ . The

$\int_{\Theta} \sigma_{ij,y_j}^1 d\Theta$ term vanishes due to periodicity and we obtain:

$$\left(\frac{1}{|\Theta|} \int_{\Theta} \sigma_{ij}^0 d\Theta \right)_{,x_j} + b_i = 0 \quad \text{on} \quad \Omega \quad (2.56)$$

Substituting the constitutive relation (2.19) and the asymptotic expansion of strain tensor (2.43) into the above equation yields the macroscopic equilibrium equation

$$\left(\frac{1}{|\Theta|} \int_{\Theta} L_{ijkl} (A_{klmn} \bar{\epsilon}_{mn} + G_{klmn} d_{mn}^{\mu} - \mu_{kl}^0) d\Theta \right)_{,x_j} + b_i = 0 \quad (2.57)$$

Finally, if we define the macroscopic stress $\bar{\sigma}_{ij}$ as

$$\bar{\sigma}_{ij} \equiv \frac{1}{|\Theta|} \int_{\Theta} \sigma_{ij}^0 d\Theta \quad (2.58)$$

then the equilibrium equations (2.56) and (2.57) can be further simplified as follows:

$$\bar{\sigma}_{ij,x_j} + b_i = 0, \quad \{ \bar{L}_{ijkl} (\bar{\epsilon}_{kl} - \bar{\mu}_{kl}) \}_{,x_j} + b_i = 0 \quad (2.59)$$

where $\bar{\mu}_{ij}$ is the overall eigenstrain given by

$$\bar{\mu}_{ij} = -\frac{1}{|\Theta|} \bar{L}_{ijkl}^{-1} \int_{\Theta} L_{klmn} (G_{mnpq} d_{pq}^{\mu} - \mu_{mn}^0) d\Theta \quad (2.60)$$

Replacing G_{mnpq} by $A_{mnpq} - I_{mnpq}$ and manipulating (2.60) with (2.38) and (2.41), the overall eigenstrain field can be expressed as

$$\bar{\mu}_{ij} = \frac{1}{|\Theta|} \int_{\Theta} B_{klij} \mu_{kl}^0 d\Theta \quad (2.61)$$

where

$$B_{ijkl} = L_{ijmn}(\mathbf{y}) A_{mnpq}(\mathbf{y}) \bar{L}_{pqkl}^{-1} \quad (2.62)$$

Equation (2.61) represents the well-known Levin's formula [32] relating the local and overall eigenstrains, and B_{ijkl} is often referred to as the elastic stress concentration function.

2.3 2-Point Scheme for Two Phase Composites

As a special case we consider a composite medium consisting of two phases, matrix and reinforcement, with respective volume fractions $c^{(m)}$ and $c^{(f)}$ such that $c^{(m)} + c^{(f)} = 1$. Superscripts m and f represent matrix and reinforcement phases, respectively. $\Theta^{(m)}$ and $\Theta^{(f)}$ denote the matrix and reinforcement domains such that $\Theta = \Theta^{(m)} \cup \Theta^{(f)}$. We assume that eigenstrains and elastic strain concentration factors are constant within each phase. This yields the simplest variant of (2.51) and (2.52) where $n = 2$. The corresponding approximation scheme is termed as the 2-point model. The overall elastic properties are given by [14]

$$\bar{L}_{ijkl} = \sum_{r=m}^f c^{(r)} L_{ijmn}^{(r)} (I_{mnkl} + G_{mnkl}^{(r)}) \quad (2.63)$$

and the overall stress reduces to:

$$\bar{\sigma}_{ij} = c^{(m)} \sigma_{ij}^{(m)} + c^{(f)} \sigma_{ij}^{(f)} \quad (2.64)$$

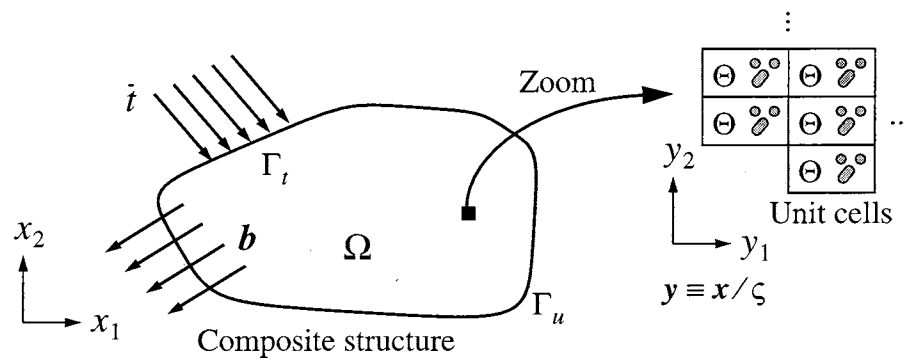


Figure 2.1 Macroscopic and microscopic structures

CHAPTER 3

THE 2-POINT SCHEME FOR FINITE DEFORMATION PLASTICITY

For finite deformation analysis the left superscript denotes the configuration: ${}^{t+\Delta t}\square$ is the current configuration at time $t + \Delta t$, whereas ${}^t\square$ is the configuration at time t . For simplicity, we will often omit the left superscript for the current configuration, i.e., $\square \equiv {}^{t+\Delta t}\square$.

3.1 Basic Assumptions

To extend the small deformation formulation to account for finite deformation effects the following assumptions are made:

A1: Phase stress objectivity

We will assume that the principle of objectivity is satisfied for each phase. Then the Cauchy stress rate for phase r is given as:

$$\dot{\sigma}_{ij}^{(r)} = \overset{\circ}{\sigma}_{ij}^{(r)} + \hat{\sigma}_{ij}^{(r)} \quad \text{where} \quad \hat{\sigma}_{ij}^{(r)} = \Lambda_{ik}^{(r)} \sigma_{kj}^{(r)} - \sigma_{ik}^{(r)} \Lambda_{kj}^{(r)} \quad (3.1)$$

where the superposed dot represents the material time derivative. The rate of deformation and spin tensor components, denoted as $\dot{\epsilon}_{ij}^{\zeta(r)}$ and $\dot{\omega}_{ij}^{\zeta(r)}$, respectively, are defined as

$$\dot{\epsilon}_{ij}^{\zeta(r)}(\mathbf{x}) \equiv v_{(i;x_j)}^{\zeta(r)} \quad \text{and} \quad \dot{\omega}_{ij}^{\zeta(r)}(\mathbf{x}) \equiv v_{[i;x_j]}^{\zeta(r)} \quad (3.2)$$

where $v_{i;x_j}^{\zeta(r)}$ is the phase velocity gradient. The asymptotic expansion of the phase velocity is given as

$$v_i^{\zeta(r)}(\mathbf{x}) \equiv v_i^{\zeta(r)}(\mathbf{x}, \mathbf{y}) \approx v_i^{0(r)}(\mathbf{x}, \mathbf{y}) + \zeta v_i^{1(r)}(\mathbf{x}, \mathbf{y}) + \dots \quad (3.3)$$

$\overset{\circ}{\sigma}_{ij}^{(r)}$ is the objective rate of the Cauchy stress in phase r , which represents the material response due to deformation, whereas $\Lambda_{ij}^{(r)} = \mathfrak{R}_{ik}^{(r)} \{ \mathfrak{R}_{kj}^{(r)} \}^{-1}$ represents the rate of rotation.

Remark (1): The choice of rotation $\mathfrak{R}_{ij}^{(r)}$ depends on the microstructure. For fibrous composites it is natural to assume that $\mathfrak{R}_{ij}^{(r)}$, represents the fiber rotation from the configuration aligned along the unit vector ${}^t m_i$ to the current configuration aligned along the vector m_i . Thus

$$m_i = \mathfrak{R}_{ij}^{(r)} {}^t m_j \quad \text{and} \quad \dot{m}_i = \dot{\mathfrak{R}}_{ip}^{(r)} \{\mathfrak{R}_{pj}^{(r)}\}^{-1} m_j \equiv \bar{\Lambda}_{ij}^{(r)} m_j \quad (3.4)$$

Following Lee [29] it can be shown that $\bar{\Lambda}_{ij}^{(r)}$ is related to the spin and rate of deformation tensors by:

$$\bar{\Lambda}_{ij}^{(r)} = \dot{\omega}_{ij}^{(r)} + \dot{\epsilon}_{ik}^{(r)} m_k m_j - \dot{\epsilon}_{jk}^{(r)} m_k m_i \quad (3.5)$$

The choice of rotations in textile and particle composites is less obvious. We refer to [25] for the discussion on various choices.

A2: Additive decomposition of hypoelastic and inelastic rate of deformation

The theoretical and practical reasons favoring additive decomposition over multiplicative decomposition for fibrous composites were discussed in [37]. In the present work we adopt the additive decomposition of rate of deformation into elastic ${}_e \dot{\epsilon}_{ij}^{(r)}$ and inelastic rate of deformation $\dot{\mu}_{ij}^{(r)}$, which gives

$$\dot{\epsilon}_{ij}^{(r)} = {}_e \dot{\epsilon}_{ij}^{(r)} + \dot{\mu}_{ij}^{(r)} \quad (3.6)$$

Furthermore, we will assume the hypoelastic constitutive equation relating the objective Cauchy stress rate with rate of elastic deformation:

$$\overset{\circ}{\sigma}_{ij}^{(r)} = L_{ijkl}^{(r)} (\dot{\epsilon}_{kl}^{(r)} - \dot{\mu}_{kl}^{(r)}) \quad (3.7)$$

A3: Midpoint integration scheme for micro- and macro-coordinates

In a typical time step $t + \Delta t$, the configuration of the macro- and micro-structure may be expressed as a sum of the configuration at the previous step t and the displacement increment:

$${}^{t+\Delta t}x_i = {}^t x_i + \Delta u_i^0 \quad (3.8)$$

$${}^{t+\Delta t}y_i = {}^t y_i + \Delta \hat{u}_i \quad (3.9)$$

The macroscopic displacement increment Δu_i^0 is found from the incremental solution of the macro-problem, whereas displacement increment in the RVE is given by:

$$\Delta \hat{u}_i(\mathbf{x}, \mathbf{y}) = \{\Delta \bar{\varepsilon}_{ij}(\mathbf{x}) + \Delta \bar{\omega}_{ij}(\mathbf{x})\}y_j + \Delta u_i^1(\mathbf{x}, \mathbf{y}) \quad (3.10)$$

The first term in (3.10) represents the contribution of macroscopic solution, whereas the second term $\Delta u_i^1(\mathbf{x}, \mathbf{y})$ accounts for oscillatory Y-periodic field. Figure 3.1 schematically illustrates the decomposition of the deformation field in the RVE.

Strain and rotation increments are integrated using the midpoint rule to obtain a second order accuracy:

$$\Delta \bar{\varepsilon}_{ij} = \frac{1}{2} \left(\frac{\partial \Delta u_i^0}{\partial {}^{t+\Delta t/2}x_j} + \frac{\partial \Delta u_j^0}{\partial {}^{t+\Delta t/2}x_i} \right) \quad (3.11)$$

$$\Delta \bar{\omega}_{ij} = \frac{1}{2} \left(\frac{\partial \Delta u_i^0}{\partial {}^{t+\Delta t/2}x_j} - \frac{\partial \Delta u_j^0}{\partial {}^{t+\Delta t/2}x_i} \right) \quad (3.12)$$

where the midpoint coordinates are defined as

$${}^{t+\Delta t/2}x_i \equiv \frac{1}{2}({}^t x_i + {}^{t+\Delta t}x_i) \quad (3.13)$$

$${}^{t+\Delta t/2}y_i \equiv \frac{1}{2}({}^t y_i + {}^{t+\Delta t}y_i) \quad (3.14)$$

Similarly, the periodic portion of the solution increment Δu_i^1 is obtained by integrating (2.30) using the midpoint rule:

$$\Delta u_i^1 = H_{imn}({}^{t+\Delta t/2}\mathbf{y})(\Delta \bar{\varepsilon}_{mn}(\mathbf{x}) + \Delta d_{mn}^u(\mathbf{x})) \quad (3.15)$$

where the increment of inelastic strain is defined in Chapters 4

A4: Additive decomposition of material and rotational response

There are several formulations aimed at extending the small deformation formulation to account for large deformation effects. One of the most popular approaches is known as the co-rotational method where all the fields of interest are transformed into the rotated \mathfrak{R} -system [25]. In the \mathfrak{R} -system, the form of constitutive equations is analogous to small deformation theory. A simpler approach, proposed by Hallquist [21] and improved by Hughes and Winget [26] to preserve incremental objectivity, is based on the additive incremental decomposition of material and rotational response. The latter procedure is adopted in the present work.

For two phase material, the integration scheme [25] decomposes stresses and back stresses as follows:

$${}^{t+\Delta t}\sigma_{ij}^{(r)} = {}^t\hat{\sigma}_{ij}^{(r)} + \Delta\sigma_{ij}^{(r)}, \quad {}^t\hat{\sigma}_{ij}^{(r)} = \mathfrak{R}_{ki}^{(r)} {}^t\sigma_{kl}^{(r)} \mathfrak{R}_{lj}^{(r)} \quad (3.16)$$

$${}^{t+\Delta t}\alpha_{ij}^{(r)} = {}^t\hat{\alpha}_{ij}^{(r)} + \Delta\alpha_{ij}^{(r)}, \quad {}^t\hat{\alpha}_{ij}^{(r)} = \mathfrak{R}_{ki}^{(r)} {}^t\alpha_{kl}^{(r)} \mathfrak{R}_{lj}^{(r)} \quad (3.17)$$

where $\alpha_{ij}^{(r)}$ is the back stress. The midpoint rule is utilized to compute the phase rotations [25]

$$\mathfrak{R}_{ij}^{(r)} = \delta_{ij} + \left(\delta_{ik} - \frac{1}{2}\Delta\omega_{ik}^{(r)} \right)^{-1} \Delta\omega_{kj}^{(r)} \quad (3.18)$$

Remark (2): For homogeneous materials the integration scheme [25] uncouples the material and rotational responses. In the present formulation phase rotations in each phase, $\mathfrak{R}_{ij}^{(r)}$, depend on phase eigenstrains, which are unknown prior to stress integration, and thus material and rotational responses are fully coupled and have to be updated simultaneously.

A5: Constant phase volume fractions

For the 2-point scheme derived in this chapter we will assume that phase volume fractions remain constant throughout the analysis. This is apparently true in the case of elastic fibers undergoing small strains and incompressible matrix material. In addition, we assume that the elastic properties of the phases are independent of temperature. Based on the first-order approximation methods, such as the Mori-Tanaka method [35] and Self Consistent method [23], the strain concentration factors and eigenstrain influence functions can be assumed to be constants throughout the entire analysis. These assumptions will allow us to carry out the entire analysis without

updating the configuration of the unit cells. For the n -point scheme model, described in Chapter 4, these restrictions will be removed.

3.2 Implicit Integration of Constitutive Equation

For the elastically deforming reinforcement the only source of eigenstrain rate is due to temperature effects, i.e., $\dot{\mu}_{ij}^{(f)} = \theta \dot{\epsilon}_{ij}^{(f)}$ where $\theta \dot{\epsilon}_{ij}^{(f)}$ is the thermal rate of deformation in reinforcement domain. The eigenstrain rate in the matrix phase is comprised of both the thermal, $\theta \dot{\epsilon}_{ij}^{(m)}$, and the plastic, ${}_p \dot{\epsilon}_{ij}^{(m)}$, rate of deformation effects, such that $\dot{\mu}_{ij}^{(m)} = \theta \dot{\epsilon}_{ij}^{(m)} + {}_p \dot{\epsilon}_{ij}^{(m)}$. The phase thermal rate of deformation can be expressed as

$$\theta \dot{\epsilon}_{ij}^{(r)} = \xi_{ij}^{(r)} \dot{\theta} \quad (3.19)$$

where θ denotes the temperature and $\xi_{ij}^{(r)}$ are components of the phase thermal expansion tensor.

Combining the rate form of (2.51), (3.7), (3.8), (3.16) and Assumptions 3 and 4 it can be shown that the following relations for the phase stresses hold:

$${}^{t+\Delta t} \sigma_{ij}^{(r)} = {}^t \hat{\sigma}_{ij}^{(r)} + R_{ijkl}^{(r)} \Delta \bar{\epsilon}_{kl} - \sum_{s=m}^f Q_{ijkl}^{(rs)} \Delta \mu_{kl}^{(s)}, \quad r = m, f \quad (3.20)$$

where $\Delta \mu_{kl}^{(s)}$ is the overall phase eigenstrain increment to be defined later in this section and

$$\left. \begin{aligned} R_{ijkl}^{(r)} &= L_{ijpq}^{(r)} (I_{pqkl} + G_{pqkl}^{(r)}) \\ Q_{ijkl}^{(rs)} &= L_{ijpq}^{(r)} (\delta_{rs} I_{pqkl} - D_{pqkl}^{(rs)}) \end{aligned} \right\} \quad r, s = m, f \quad (3.21)$$

Consider the yield function of the following form:

$$\Phi^{(m)}(\sigma_{ij}^{(m)} - \alpha_{ij}^{(m)}, Y^{(m)}) = \frac{1}{2} (\sigma_{ij}^{(m)} - \alpha_{ij}^{(m)}) P_{ijkl} (\sigma_{kl}^{(m)} - \alpha_{kl}^{(m)}) - \frac{1}{3} \{Y^{(m)}\}^2 \quad (3.22)$$

where $Y^{(m)}$ is the yield stress of the matrix phase in a uniaxial test, which evolves according to the hardening laws assumed; $\alpha_{ij}^{(m)}$ corresponds to the center of the yield surface in the deviatoric

stress space, or simply the back stress. Evolution of the back stress is assumed to follow the kinematic hardening rule. For von Mises plasticity, P_{ijkl} is a projection operator which transforms an arbitrary second order tensor to the deviatoric space:

$$P_{ijkl} = I_{ijkl} - \frac{1}{3}\delta_{ij}\delta_{kl} \quad (3.23)$$

For simplicity we assume that the plastic rate of deformation in the matrix phase follows the associative flow rule:

$${}_p\dot{\varepsilon}_{ij}^{(m)} = \frac{\partial\Phi}{\partial\sigma_{ij}^{(m)}}\dot{\lambda}^{(m)} = \mathfrak{K}_{ij}^{(m)}\dot{\lambda}^{(m)}, \quad \mathfrak{K}_{ij}^{(m)} = P_{ijkl}(\sigma_{kl}^{(m)} - \alpha_{kl}^{(m)}) \quad (3.24)$$

We adopt a modified version of the hardening evolution law [25] in the context of isotropic, homogeneous, elasto-plastic matrix phase. A scalar material dependent parameter β ($0 \leq \beta \leq 1$) is used as a measure of the proportion of isotropic and kinematic hardening and $\lambda^{(m)}$ is a plastic parameter to be determined by the consistency condition (3.22). Accordingly, the evolution of the yield stress $Y^{(m)}$ and the back stress $\alpha_{ij}^{(m)}$ can be expressed as follows:

$$\dot{Y}^{(m)} = \frac{2\beta h}{3}Y^{(m)}\dot{\lambda}^{(m)} \quad (3.25)$$

$$\dot{\alpha}_{ij}^{(m)} = \frac{2(1-\beta)h}{3}P_{ijkl}(\sigma_{kl}^{(m)} - \alpha_{kl}^{(m)})\dot{\lambda}^{(m)} \quad (3.26)$$

where $\beta = 0$ corresponds to a pure isotropic hardening; $\beta = 1$ is the widely used Ziegler-Prager kinematic hardening rule [48] for metals; h is a hardening parameter defined as the ratio between effective stress rate and the effective plastic strain rate.

Integration of (3.24), (3.25) and (3.26) is carried out using the backward Euler scheme:

$${}^{t+\Delta t}{}_p\varepsilon_{ij}^{(m)} = {}^t{}_p\varepsilon_{ij}^{(m)} + {}^{t+\Delta t}\mathfrak{K}_{ij}^{(m)}\Delta\lambda^{(m)} \quad (3.27)$$

$${}^{t+\Delta t}Y^{(m)} = {}^tY^{(m)} + \frac{2\beta h}{3}{}^{t+\Delta t}Y^{(m)}\Delta\lambda^{(m)} \quad (3.28)$$

$${}^{t+\Delta t}\alpha_{ij}^{(m)} = {}^t\hat{\alpha}_{ij}^{(m)} + \frac{2(1-\beta)h}{3}P_{ijkl}({}^{t+\Delta t}\sigma_{kl}^{(m)} - {}^{t+\Delta t}\alpha_{kl}^{(m)})\Delta\lambda^{(m)} \quad (3.29)$$

where $\Delta\lambda^{(m)} \equiv {}^{t+\Delta t}\lambda^{(m)} - {}^t\lambda^{(m)}$, and ${}^t\hat{\alpha}_{ij}^{(m)}$ is the rotated back stress defined in (3.17). The phase rotation increment follows from (2.52), (3.19) and (3.24):

$$\Delta\omega_{ij}^{(r)} = \Delta\bar{\omega}_{ij} + \hat{G}_{ijkl}^{(r)}\Delta\bar{\epsilon}_{kl} + \hat{D}_{ijkl}^{(rm)}P_{klmn}(\sigma_{mn}^{(m)} - \alpha_{mn}^{(m)})\Delta\lambda^{(m)} + \sum_{s=m}^f \hat{D}_{ijkl}^{(rs)}\xi_{kl}^{(s)}\Delta\theta \quad (3.30)$$

In the following we omit the left superscript for the current step $t + \Delta t$. Using the backward Euler scheme for the rate form of $\sigma_{ij}^{(m)}$ in (3.20) and (3.27) yields the following relation for the Cauchy stress in the matrix domain:

$$\sigma_{ij}^{(m)} = {}_{tr}\sigma_{ij}^{(m)} - Q_{ijkl}^{(mm)}\kappa_{kl}^{(m)}\Delta\lambda^{(m)} \quad (3.31)$$

where ${}_{tr}\sigma_{ij}^{(m)}$ is a trial Cauchy stress in the matrix phase defined as

$${}_{tr}\sigma_{ij}^{(m)} \equiv {}^t\hat{\sigma}_{ij}^{(m)} + R_{ijkl}^{(m)}\Delta\bar{\epsilon}_{kl} - \sum_{s=m}^f Q_{ijkl}^{(ms)}\xi_{kl}^{(s)}\Delta\theta \quad (3.32)$$

The process is termed elastic if:

$$({}_{tr}\sigma_{ij}^{(m)} - \alpha_{ij}^{(m)})P_{ijkl}({}_{tr}\sigma_{kl}^{(m)} - \alpha_{kl}^{(m)}) - \frac{2}{3}\{Y^{(m)}\}^2 \Big|_{\Delta\lambda^{(m)}=0} < 0 \quad (3.33)$$

Otherwise the process is plastic, which is the focus of our subsequent derivation.

Subtracting (3.29) from (3.31) we arrive at the following result:

$$\sigma_{ij}^{(m)} - \alpha_{ij}^{(m)} = (I_{ijkl} + \Delta\lambda^{(m)}\wp_{ijkl})^{-1}({}_{tr}\sigma_{kl}^{(m)} - {}^t\hat{\alpha}_{kl}^{(m)}) \quad (3.34)$$

where

$$\wp_{ijkl} = Q_{ijst}^{(mm)}P_{stkl} + \frac{2}{3}(1-\beta)hP_{ijkl} \quad (3.35)$$

The value of $\Delta\lambda^{(m)}$ is obtained by satisfying the consistency condition which assures that the stress state in the plastic process lies on the yield surface at the end of the current load step. To this end, equations (3.28) and (3.34) are substituted into the yield condition (3.22), $\Phi^{(m)}(\sigma_{ij}^{(m)} - \alpha_{ij}^{(m)}, Y^{(m)}) = 0$, which produces a nonlinear equation for $\Delta\lambda^{(m)}$. A standard Newton's method is applied to solve for $\Delta\lambda^{(m)}$:

$$\Delta\lambda_{k+1}^{(m)} = \Delta\lambda_k^{(m)} - \left\{ \frac{\partial\Phi^{(m)}}{\partial\Delta\lambda^{(m)}} \right\}^{-1} \Phi^{(m)} \Big|_{\Delta\lambda_k^{(m)}} \quad (3.36)$$

where k is the iteration count. It can be shown that the derivative $\partial\Phi^{(m)}/\partial\Delta\lambda^{(m)}$ required in (3.36) has the following form:

$$\frac{\partial\Phi^{(m)}}{\partial\Delta\lambda^{(m)}} = \mathfrak{N}_{ij}^{(m)} C_{ijkl}^{(m)} (\sigma_{kl}^{(m)} - \alpha_{kl}^{(m)}) - \frac{4\beta h \{Y^{(m)}\}^2}{9 - 6\beta h \Delta\lambda^{(m)}} \quad (3.37)$$

The expression for $C_{ijkl}^{(m)}$ is derived in Appendix A. The converged value of $\Delta\lambda^{(m)}$ is then used to compute the phase stresses. The overall stress is computed from (2.64).

3.3 Consistent Linearization

While integration of the constitutive equations affects the accuracy of the solution, the formation of a tangent stiffness matrix consistent with the integration procedure is essential to maintain the quadratic rate of convergence if one is to adopt the Newton method for the solution of nonlinear system of equations on the macro level [43].

The starting point is the incremental form of the constitutive equations (3.20):

$$\sigma_{ij}^{(r)} = {}^t\hat{\sigma}_{ij}^{(r)} + R_{ijkl}^{(r)} \Delta\bar{\epsilon}_{kl} - Q_{ijkl}^{(rm)} \mathfrak{N}_{kl}^{(m)} \Delta\lambda^{(m)} - \sum_{s=m}^f Q_{ijkl}^{(rs)} \xi_{kl}^{(s)} \Delta\theta \quad (3.38)$$

Taking material time derivative of (3.29), (3.30) and (3.38) yields:

$$\dot{\alpha}_{ij}^{(m)} = \dot{\hat{\alpha}}_{ij}^{(m)} + \frac{2(1-\beta)h}{3} \{ \mathfrak{N}_{ij}^{(m)} \dot{\lambda}^{(m)} + P_{ijpq} (\dot{\sigma}_{pq}^{(m)} - \dot{\alpha}_{pq}^{(m)}) \Delta\lambda^{(m)} \} \quad (3.39)$$

$$\begin{aligned}\Delta\dot{\omega}_{ij}^{(r)} &= \Delta\dot{\bar{\omega}}_{ij} + \hat{G}_{ijkl}^{(r)}\Delta\dot{\bar{\epsilon}}_{kl} + \hat{D}_{ijkl}^{(rm)}\{\mathfrak{N}_{kl}^{(m)}\dot{\lambda}^{(m)} + P_{klpq}(\dot{\sigma}_{pq}^{(m)} - \dot{\alpha}_{pq}^{(m)})\Delta\lambda^{(m)}\} \\ &\quad + \sum_{s=m}^f \hat{D}_{ijkl}^{(rs)}\xi_{kl}^{(s)}\dot{\theta}\end{aligned}\quad (3.40)$$

$$\begin{aligned}\dot{\sigma}_{ij}^{(r)} &= {}^t\dot{\bar{\sigma}}_{ij}^{(r)} + R_{ijkl}^{(r)}\Delta\dot{\bar{\epsilon}}_{kl} - Q_{ijkl}^{(rm)}\{\mathfrak{N}_{kl}^{(m)}\dot{\lambda}^{(m)} + P_{klpq}(\dot{\sigma}_{pq}^{(m)} - \dot{\alpha}_{pq}^{(m)})\Delta\lambda^{(m)}\} \\ &\quad - \sum_{s=m}^f Q_{ijkl}^{(rs)}\xi_{kl}^{(s)}\dot{\theta}\end{aligned}\quad (3.41)$$

Subtracting (3.39) from (3.41) for $r = m$ yields:

$$\begin{aligned}\dot{\sigma}_{ij}^{(m)} - \dot{\alpha}_{ij}^{(m)} &= {}^t\dot{\bar{\sigma}}_{ij}^{(m)} - {}^t\dot{\bar{\alpha}}_{ij}^{(m)} + R_{ijkl}^{(m)}\Delta\dot{\bar{\epsilon}}_{kl} - \sum_{s=m}^f Q_{ijkl}^{(ms)}\xi_{kl}^{(s)}\dot{\theta} \\ &\quad - \wp_{ijkl}\{(\sigma_{kl}^{(m)} - \alpha_{kl}^{(m)})\dot{\lambda}^{(m)} + (\dot{\sigma}_{kl}^{(m)} - \dot{\alpha}_{kl}^{(m)})\Delta\lambda^{(m)}\}\end{aligned}\quad (3.42)$$

where

$${}^t\dot{\bar{\sigma}}_{ij}^{(m)} - {}^t\dot{\bar{\alpha}}_{ij}^{(m)} = \frac{\partial(\hat{\sigma}_{ij}^{(m)} - \hat{\alpha}_{ij}^{(m)})}{\partial\Delta\omega_{kl}^{(m)}}\Delta\dot{\omega}_{kl}^{(m)}\quad (3.43)$$

Combining (3.40), (3.42), (3.43), (A.8) and (A.9) with the consistent linearizations of $\Delta\dot{\bar{\epsilon}}_{kl}$ and $\Delta\dot{\bar{\omega}}_{kl}$ (given in Appendix B (B.11)) yields:

$$\dot{\sigma}_{ij}^{(m)} - \dot{\alpha}_{ij}^{(m)} = (I_{ijkl} + \Delta\lambda^{(m)}W_{ijkl}^{(m)})^{-1}({}_vS_{klst}v_{s,x_t}^0 + \theta S_{kl}\dot{\theta} + \lambda S_{kl}\dot{\lambda}^{(m)})\quad (3.44)$$

where

$${}_vS_{klst} = (\sigma_{klmn}^{(m)} - \alpha_{klmn}^{(m)})(M_{[mn]st} + \hat{G}_{mnuv}M_{(uv)st}) + R_{klmn}M_{(mn)st}\quad (3.45)$$

$$\theta S_{kl} = \sum_{s=m}^f \{(\sigma_{klpq}^{(m)} - \alpha_{klpq}^{(m)})\hat{D}_{pqst}^{(ms)} - Q_{klst}^{(ms)}\}\xi_{st}^{(s)}\quad (3.46)$$

$$\lambda S_{kl} = -W_{klst}^{(m)}(\sigma_{st}^{(m)} - \alpha_{st}^{(m)})\quad (3.47)$$

and $W_{ijkl}^{(m)}$, $\sigma_{klmn}^{(m)}$ and $\alpha_{klmn}^{(m)}$ are defined in (A.13), (A.8) and (A.9), respectively. It remains to eliminate $\dot{\lambda}^{(m)}$ from (3.44), by utilizing the linearized form of the consistency condition (3.22) and equation (3.28) which gives

$$\mathfrak{N}_{ij}^{(m)}(\dot{\sigma}_{ij}^{(m)} - \dot{\alpha}_{ij}^{(m)}) - \frac{4\beta h \{Y^{(m)}\}^2 \dot{\lambda}^{(m)}}{9 - 6\beta h \Delta \lambda^{(m)}} = 0 \quad (3.48)$$

Substituting (3.44) into (3.48) results in

$$\dot{\lambda}^{(m)} = \Gamma_{kl}^{(m)} (\nu S_{klst} v_{s, x_t}^0 + \theta S_{kl} \dot{\theta}) \quad (3.49)$$

where

$$\Gamma_{kl}^{(m)} = \frac{(9 - 6\beta h \Delta \lambda^{(m)}) \mathfrak{N}_{ij}^{(m)} (I_{ijkl} + \Delta \lambda^{(m)} W_{ijkl}^{(m)})^{-1}}{4\beta h \{Y^{(m)}\}^2 - (9 - 6\beta h \Delta \lambda^{(m)}) \mathfrak{N}_{mn}^{(m)} (I_{mnst} + \Delta \lambda^{(m)} W_{mnst}^{(m)})^{-1} \lambda S_{st}} \quad (3.50)$$

and thus (3.44) can be simplified as

$$\dot{\sigma}_{ij}^{(m)} - \dot{\alpha}_{ij}^{(m)} = \nu S_{ijkl} v_{k, x_l}^0 + \theta S_{ij} \dot{\theta} \quad (3.51)$$

where

$$\nu S_{ijkl} = (I_{ijmn} + \Delta \lambda^{(m)} W_{ijmn}^{(m)})^{-1} (\nu S_{mnkl} + \lambda S_{mn} \Gamma_{pq}^{(m)} \nu S_{pqkl}) \quad (3.52)$$

$$\theta S_{ij} = (I_{ijmn} + \Delta \lambda^{(m)} W_{ijmn}^{(m)})^{-1} (\theta S_{mn} + \lambda S_{mn} \Gamma_{pq}^{(m)} \theta S_{pq}) \quad (3.53)$$

Finally, by substituting (3.49), (3.51), (A.8) and (B.11) into (3.41), we get a closed form expression relating the phase Cauchy stress rate $\dot{\sigma}_{ij}^{(r)}$ with the macroscopic velocity gradient v_{k, x_l}^0 and the temperature rate $\dot{\theta}$

$$\dot{\sigma}_{ij}^{(r)} = D_{ijkl}^{(r)} v_{k, x_l}^0 + d_{ij}^{(r)} \dot{\theta} \quad (3.54)$$

where

$$\begin{aligned}
D_{ijkl}^{(r)} &= R_{ijmn}^{(r)} M_{(mn)kl} + \sigma U_{ijpq}^{(r)} (M_{[pq]kl} + \hat{G}_{pqmn}^{(r)} M_{(mn)kl}) \\
&\quad + (\sigma U_{ijpq}^{(r)} \hat{D}_{pqmn} - Q_{ijmn}^{(rm)}) (\mathfrak{K}_{mn}^{(m)} \Gamma_{uv}^{(m)} \nu_{uvkl} + \Delta\lambda^{(m)} P_{mnpq} \nu_{pqkl})
\end{aligned} \tag{3.55}$$

and

$$\begin{aligned}
d_{ij}^{(r)} &= \sum_{s=m}^f (\sigma U_{ijpq}^{(r)} \hat{D}_{pqkl}^{(rs)} - Q_{ijkl}^{(rs)}) \xi_{kl}^{(s)} \\
&\quad + (\sigma U_{ijpq}^{(r)} \hat{D}_{pqmn} - Q_{ijmn}^{(rm)}) (\mathfrak{K}_{mn}^{(m)} \Gamma_{pq}^{(m)} \theta_{pq} + \Delta\lambda^{(m)} P_{mnpq} \theta_{pq})
\end{aligned} \tag{3.56}$$

The overall consistent instantaneous stiffness D_{ijkl} is obtained from the rate form of (2.64) and Assumption A5:

$$\dot{\bar{\sigma}}_{ij} = D_{ijkl} v_{k, x_l}^0 + d_{ij} \dot{\theta} \tag{3.57}$$

where

$$D_{ijkl} = c^{(m)} D_{ijkl}^{(m)} + c^{(f)} D_{ijkl}^{(f)}, \quad d_{ij} = c^{(m)} d_{ij}^{(m)} + c^{(f)} d_{ij}^{(f)} \tag{3.58}$$

The overall consistent tangent operator is derived from the consistent linearization of the weak form of the macroscopic equilibrium equation (2.59). Consider the internal force vector expressed in terms of the quantities defined in the deformed configuration

$$f_A^{int} = \int_{\Omega} N_{iA, x_j} \bar{\sigma}_{ij} d\Omega \tag{3.59}$$

where N_{iA} is a set of shape functions in the macroscale.

Prior to linearization, the internal force vector is defined in the reference configuration ${}^t\Omega$ as

$$f_A^{int} = \int_{{}^t\Omega} N_{iA, {}^t x_m} F_{mj}^{-1} \bar{\sigma}_{ij} J_x d{}^t\Omega \tag{3.60}$$

where J_x is the jacobian between the macro-configurations at times t and $t + \Delta t$; F_{jm} is the macroscopic deformation gradient defined as

$$F_{jm} = x_{j, x_m} \equiv {}^{t+\Delta t}x_{j, x_m} \quad \text{and} \quad F_{mj}^{-1} = {}^t x_{m, x_j} \equiv {}^t x_{m, t+\Delta t, x_j} \quad (3.61)$$

Linearization of (3.60) yields

$$\frac{d}{dt} f_A^{int} = \int_{\Omega} N_{iA, x_m} \{ \dot{F}_{mj}^{-1} \bar{\sigma}_{ij} J_x + F_{mj}^{-1} \dot{\bar{\sigma}}_{ij} J_x + F_{mj}^{-1} \bar{\sigma}_{ij} \dot{J}_x \} d^t \Omega \quad (3.62)$$

Substituting (3.57) into (3.62) and exploiting the kinematical relations $\dot{J}_x = J_x v_{k, x_k}^0$,

$\dot{F}_{mj}^{-1} = -F_{ml}^{-1} v_{l, x_j}^0$ and the finite element discretization $v_{k, x_l}^0 = N_{kB, x_l} \dot{q}_B$ yields:

$$\frac{d}{dt} f_A^{int} = \int_{\Omega} N_{iA, x_j} \bar{D}_{ijkl} N_{kB, x_l} d\Omega \dot{q}_B + \int_{\Omega} N_{iA, x_j} d_{ij} d\Omega \dot{\theta} \quad (3.63)$$

$$\bar{D}_{ijkl} = D_{ijkl} + \delta_{kl} \bar{\sigma}_{ij} - \delta_{kj} \bar{\sigma}_{il} \quad (3.64)$$

where D_{ijkl} and d_{ij} are defined in (3.58); \dot{q}_B denotes the velocity degree of freedoms associated with the finite element mesh. The first integral in (3.63) represents the consistent tangent stiffness matrix for the macro-problem.

Remark (3): For the purpose of linearization it is convenient to approximate phase rotations within a unit cell by a constant field such that $\dot{\omega}_{ij}^{(r)} \approx \dot{\bar{\omega}}_{ij}$. The resulting rotated stress and back stress rates are given as

$$\dot{\bar{\sigma}}_{ij}^{(r)} = \Delta \dot{\bar{\omega}}_{ik} \sigma_{kj}^{(r)} - \sigma_{ik}^{(r)} \Delta \dot{\bar{\omega}}_{kj}, \quad \dot{\bar{\alpha}}_{ij}^{(m)} = \Delta \dot{\bar{\omega}}_{ik} \alpha_{kj}^{(m)} - \alpha_{ik}^{(m)} \Delta \dot{\bar{\omega}}_{kj} \quad (3.65)$$

Therefore, (3.45) to (3.47) can be simplified as

$${}^v S_{ijkl} = R_{ijmn} M_{(mn)kl} \{ \delta_{in} (\sigma_{mj}^{(m)} - \alpha_{mj}^{(m)}) + \delta_{jn} (\sigma_{im}^{(m)} - \alpha_{im}^{(m)}) \} M_{[mn]kl} \quad (3.66)$$

$$\theta S_{ij} = - \sum_{s=m}^f Q_{ijkl}^{(ms)} \xi_{kl}^{(s)} \quad (3.67)$$

$$\lambda S_{ij} = - \wp_{ijkl} (\sigma_{kl}^{(m)} - \alpha_{kl}^{(m)}) \quad (3.68)$$

and $W_{ijkl}^{(m)} = \wp_{ijkl}$ in (3.44), (3.50), (3.52) and (3.53). $D_{ijkl}^{(r)}$ and $d_{ij}^{(r)}$ in (3.55) and (3.56) are written as

$$\begin{aligned} D_{ijkl}^{(r)} = & R_{ijmn}^{(r)} M_{(mn)kl} - (\delta_{in} \sigma_{mj}^{(r)} + \delta_{jn} \sigma_{im}^{(r)}) M_{[mn]kl} \\ & - Q_{ijmn}^{(rm)} (\mathfrak{K}_{mn}^{(m)} \Gamma_{uv}^{(m)} \nu S_{uvkl} + \Delta \lambda^{(m)} P_{mnpq} \nu S_{pqkl}) \end{aligned} \quad (3.69)$$

and

$$d_{ij}^{(r)} = -Q_{ijmn}^{(rm)} (\mathfrak{K}_{mn}^{(m)} \Gamma_{pq}^{(m)} \theta S_{pq} + \Delta \lambda^{(m)} P_{mnpq} \theta S_{pq}) - \sum_{s=m}^f Q_{ijkl}^{(rs)} \xi_{kl}^{(s)} \quad (3.70)$$

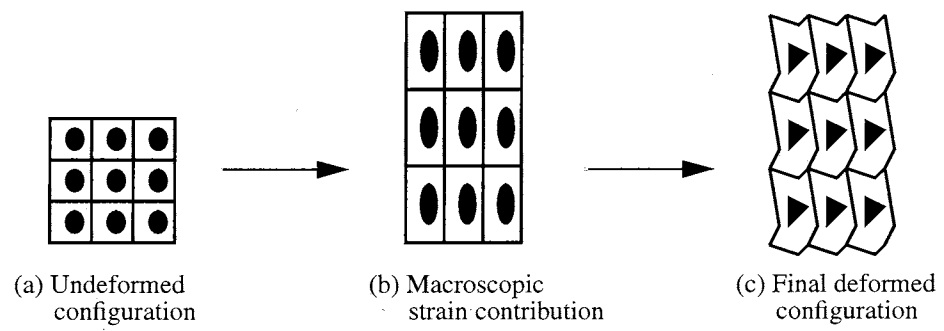


Figure 3.1 Decomposition of deformation in the microstructure

CHAPTER 4

THE n -POINT SCHEME FOR FINITE DEFORMATION PLASTICITY

In this section we consider a unit cell model discretized with n elements. The n -point scheme model assumes that eigenstrains are piecewise constant, i.e., they are constant within each element, but may vary from element to element. Our starting point (Chapter 4.1) is a rate form of the governing equations representing the finite deformation plasticity of periodic heterogeneous media. Implicit integration of constitutive equations followed by consistent linearization are presented in Chapters 4.2 and 4.3.

4.1 Governing Equations

The governing equations consist of: equilibrium (2.4), kinematics in the rate form (3.2), boundary conditions (2.8), (2.9), and the constitutive equation in the rate form

$$\dot{\sigma}_{ij}^{\zeta} = \overset{\circ}{\sigma}_{ij}^{\zeta} + \Lambda_{ik}^{\zeta} \sigma_{kj}^{\zeta} - \sigma_{ik}^{\zeta} \Lambda_{kj}^{\zeta} \quad (4.1)$$

where

$$\overset{\circ}{\sigma}_{ij}^{\zeta} = \mathcal{L}_{ijkl}(\dot{\epsilon}_{kl}^{\zeta} - \xi_{kl}\dot{\theta}) \quad (4.2)$$

\mathcal{L}_{ijkl} denotes the instantaneous stiffness properties. In the following, we adopt Jaumann rate, i.e.,

$$\Lambda_{kj}^{\zeta} = \dot{\omega}_{kj}^{\zeta}.$$

Double scale asymptotic expansion of the velocity field (3.3) provides the starting point for the asymptotic analysis. Substituting the asymptotic expansions (2.20), (3.3) into constitutive equation (4.2) based on the Jaumann rate yields:

$$\dot{\sigma}_{ij}^s = \overset{\circ}{\sigma}_{ij}^s + \frac{1}{2} \sum_{r=-1}^s (\sigma_{il}^r \delta_{jk} + \sigma_{jl}^r \delta_{ik} - \sigma_{ik}^r \delta_{jl} - \sigma_{jk}^r \delta_{il}) l_{kl}^{s-r+1}, \quad s = -1, 0, \dots \quad (4.3)$$

where l_{kl}^s is the velocity gradient given as

$$l_{kl}^{-1} = v_{k, x_l}^0 \quad \text{and} \quad l_{kl}^s = v_{k, x_l}^{s+1} + v_{k, y_l}^s, \quad s = 0, 1, \dots \quad (4.4)$$

Further assuming that $O(\zeta^{-1})$ Cauchy stress vanishes, $\dot{\sigma}_{ij}^{-1} = \mathcal{L}_{ijkl} v_{k,y_j}^0 = 0$, yields $v_i^0 = v_i^0(\mathbf{x})$ provided that \mathcal{L}_{ijkl} is not singular. We proceed to the $O(\zeta^{-1})$ equilibrium equation (2.22):

$$\sigma_{ij,y_j}^0(\mathbf{x}, \mathbf{y}) = 0 \quad (4.5)$$

To solve for (4.5) up to a constant we introduce the following separation of variables:

$$v_i^1(\mathbf{x}, \mathbf{y}) = \mathcal{H}_{ikl}(\mathbf{y}) \{v_{k,x_l}^0(\mathbf{x}) + d_{kl}^\theta(\mathbf{x})\} \quad (4.6)$$

Note that plastic effects are now hidden in the Y-periodic function $\mathcal{H}_{ikl}(\mathbf{y})$, whereas d_{kl}^θ accounts for temperature effects only.

Pre-multiplying (4.5) by the Y-periodic function $\mathcal{H}_{ikl}(\mathbf{y})$, then integrating over the deformed unit cell domain Θ and carrying out integration by parts yields

$$\phi(\mathbf{x}, \mathbf{y}) = \int_{\Theta} \mathcal{H}_{ikl,y_j} \sigma_{ij}^0 d\Theta = 0 \quad (4.7)$$

Linearization of (4.7) is carried out by taking the material time derivative, $\dot{\phi} = 0$. For this purpose we express the integrand of (4.7) in the reference configuration, say at time t , $\mathcal{H}_{ikl,y_j} \sigma_{ij}^0 d\Theta = \mathcal{H}_{ikl,t,y_m} \mathcal{F}_{mj}^{-1} \sigma_{ij}^0 J_y d^t\Theta$ where $\mathcal{F}_{jm} = y_{j,t,y_m}$ denotes the deformation gradient in the unit cell and J_y is the corresponding jacobian. By utilizing equations (2.2) and (2.3) it can be shown that $y_{j,t,y_m} = x_{j,t,x_m}$.

Consequently, linearization of (4.7) yields:

$$\int_{\Theta} \mathcal{H}_{ikl,t,y_m} (\dot{\mathcal{F}}_{mj}^{-1} \sigma_{ij}^0 J_y + \mathcal{F}_{mj}^{-1} \dot{\sigma}_{ij}^0 J_y + \mathcal{F}_{mj}^{-1} \sigma_{ij}^0 \dot{J}_y) d^t\Theta = 0 \quad (4.8)$$

Substituting (4.2), (4.3), (4.4) and (4.6) into (4.8) and exploiting kinematical relations $\dot{J}_y = J_y I_{kk}^0$ and $\dot{\mathcal{F}}_{mj}^{-1} = -\mathcal{F}_{ml}^{-1} I_{lj}^0$ gives:

$$\int_{\Theta} \mathcal{H}_{ikl, y_j} \{ (\mathcal{L}_{ijmn} + \mathcal{T}_{ijmn}) l_{mn}^0 - \mathcal{L}_{ijmn} \xi_{mn} \dot{\theta} \} d\Theta = 0 \quad (4.9)$$

where

$$l_{mn}^0 = (\delta_{ms} \delta_{nt} + \mathcal{H}_{mst, y_n}(\mathbf{y})) v_{s, x_t}^0(\mathbf{x}) + \mathcal{H}_{mst, y_n}(\mathbf{y}) \dot{d}_{st}^\theta(\mathbf{x}) \quad (4.10)$$

$$\mathcal{T}_{ijmn} = \delta_{mn} \sigma_{ij}^0 + \frac{1}{2} (\delta_{im} \sigma_{jn}^0 - \delta_{jm} \sigma_{in}^0 - \delta_{in} \sigma_{jm}^0 - \delta_{jn} \sigma_{im}^0) \quad (4.11)$$

Since (4.9) is satisfied for arbitrary macro-fields $v_{s, x_t}^0(\mathbf{x})$ and $\dot{d}_{st}^\theta(\mathbf{x})$ we can obtain two integral equations in Θ :

$$\int_{\Theta} \mathcal{H}_{ikl, y_j} (\mathcal{L}_{ijmn} + \mathcal{T}_{ijmn}) (\delta_{ms} \delta_{nt} + \mathcal{H}_{mst, y_n}) d\Theta = 0 \quad (4.12)$$

$$\int_{\Theta} \mathcal{H}_{ikl, y_j} \{ (\mathcal{L}_{ijmn} + \mathcal{T}_{ijmn}) \mathcal{H}_{mst, y_n} \dot{d}_{st}^\theta - \mathcal{L}_{ijmn} \xi_{mn} \dot{\theta} \} d\Theta = 0 \quad (4.13)$$

Equation (4.12) is solved using the finite element method for \mathcal{H}_{ikl} . Note that equation (4.12) is solved for nine right hand side vectors corresponding to nine uniform velocity gradient fields as opposed to six constant strain modes in the case of small deformations.

After solving (4.12) for \mathcal{H}_{ikl} , \dot{d}_{ij}^θ can be obtained from (4.13) as

$$\dot{d}_{ij}^\theta = \frac{1}{|\Theta|} (\tilde{\mathcal{L}}_{ijkl} - \bar{\mathcal{L}}_{ijkl})^{-1} \int_{\Theta} \mathcal{H}_{rkl, y_s} \mathcal{L}_{rsuv} \xi_{uv} \dot{\theta} d\Theta \quad (4.14)$$

where

$$\tilde{\mathcal{L}}_{ijkl} = \frac{1}{|\Theta|} \int_{\Theta} (\mathcal{L}_{ijkl} + \mathcal{T}_{ijkl}) d\Theta \quad (4.15)$$

$$\bar{\mathcal{L}}_{ijkl} = \frac{1}{|\Theta|} \int_{\Theta} (\mathcal{L}_{ijmn} + \mathcal{T}_{ijmn}) \mathcal{H}_{mkl, y_n} d\Theta \quad (4.16)$$

Once \mathcal{H}_{ikl} and \dot{d}_{ij}^θ are computed, the $O(\zeta^0)$ approximation of $\dot{\boldsymbol{\varepsilon}}_{ij}^\zeta$ and $\dot{\boldsymbol{\omega}}_{ij}^\zeta$, denoted as $\dot{\boldsymbol{\varepsilon}}_{ij}$ and $\dot{\boldsymbol{\omega}}_{ij}$, are given as

$$\dot{\epsilon}_{ij} = \mathcal{A}_{ijkl} v_{k, x_l}^0 + a_{ij} \dot{\theta} \quad (4.17)$$

$$\dot{\omega}_{ij} = \hat{\mathcal{A}}_{ijkl} v_{k, x_l}^0 + \hat{a}_{ij} \dot{\theta} \quad (4.18)$$

where

$$\mathcal{A}_{ijkl}(\mathbf{y}) = \frac{1}{2}(\delta_{ik}\delta_{jl} + \delta_{jk}\delta_{il}) + \mathcal{H}_{(i, y)kl}(\mathbf{y}) \quad (4.19)$$

$$\hat{\mathcal{A}}_{ijkl}(\mathbf{y}) = \frac{1}{2}(\delta_{ik}\delta_{jl} - \delta_{jk}\delta_{il}) + \mathcal{H}_{[i, y]kl}(\mathbf{y}) \quad (4.20)$$

$$a_{ij} = \mathcal{H}_{(i, y)kl}(\tilde{\mathcal{L}}_{klpq} - \bar{\mathcal{L}}_{klpq})^{-1} \int_{\Theta} \mathcal{H}_{prqs, y_q} \mathcal{L}_{rsuv} \xi_{uv} \dot{\theta} d\Theta \quad (4.21)$$

$$\hat{a}_{ij} = \mathcal{H}_{[i, y]kl}(\tilde{\mathcal{L}}_{klpq} - \bar{\mathcal{L}}_{klpq})^{-1} \int_{\Theta} \mathcal{H}_{prqs, y_q} \mathcal{L}_{rsuv} \xi_{uv} \dot{\theta} d\Theta \quad (4.22)$$

4.2 Implicit Integration of Constitutive Equations

We start from the constitutive relation for a typical element ρ in Θ :

$$\overset{\circ}{\sigma}_{ij}^{(\rho)} = \begin{cases} L_{ijkl}^{(\rho)}(\dot{\epsilon}_{kl}^{(\rho)} - \xi_{kl}^{(\rho)}\dot{\theta}) & \text{if } \rho \in \Theta^{(f)} \\ L_{ijkl}^{(\rho)}(\dot{\epsilon}_{kl}^{(\rho)} - \xi_{kl}^{(\rho)}\dot{\theta} - \rho \dot{\epsilon}_{kl}^{(\rho)}) & \text{if } \rho \in \Theta^{(m)} \end{cases} \quad (4.23)$$

For elements in the matrix phase (4.23) can be written as

$$\overset{\circ}{\sigma}_{ij}^{(\rho)} = L_{ijkl}^{(\rho)} \{ \mathcal{A}_{klmn}^{(\rho)} v_{m, x_n}^0 + (a_{kl}^{(\rho)} - \xi_{kl}^{(\rho)})\dot{\theta} - \mathfrak{K}_{kl}^{(\rho)} \dot{\lambda}^{(\rho)} \} \quad (4.24)$$

Applying the backward Euler integration scheme to (4.24) gives

$$\sigma_{ij}^{(\rho)} = {}^t \hat{\sigma}_{ij}^{(\rho)} + L_{ijkl}^{(\rho)} \{ \mathcal{A}_{klmn}^{(\rho)} (\Delta \bar{\epsilon}_{mn} + \Delta \bar{\omega}_{mn}) + (a_{kl}^{(\rho)} - \xi_{kl}^{(\rho)}) \Delta \theta - \mathfrak{K}_{kl}^{(\rho)} \Delta \lambda^{(\rho)} \} \quad (4.25)$$

and exploiting the equation for the back stress in element ρ (3.29) yields

$$\sigma_{ij}^{(\rho)} - \alpha_{ij}^{(\rho)} = (I_{ijmn} + \Delta \lambda^{(\rho)} \mathcal{Q}_{ijmn}^{(\rho)})^{-1} \mathfrak{Z}_{mn}^{(\rho)} \quad (4.26)$$

where

$$\mathcal{Q}_{ijmn}^{(\rho)} = L_{ijuv}^{(\rho)} P_{uvmn} + \frac{2}{3}(1 - \beta)hP_{ijmn} \quad (4.27)$$

$$\mathfrak{Z}_{mn}^{(\rho)} = {}^t\hat{\sigma}_{mn}^{(\rho)} - {}^t\hat{\alpha}_{mn}^{(\rho)} - L_{mnpq}^{(\rho)} \{ \mathcal{A}_{pqst}^{(\rho)} (\Delta\bar{\epsilon}_{st} + \Delta\bar{\omega}_{st}) + (a_{pq}^{(\rho)} - \xi_{pq}^{(\rho)}) \Delta\theta \} \quad (4.28)$$

in which ${}^t\hat{\sigma}_{mn}^{(\rho)}$ and ${}^t\hat{\alpha}_{mn}^{(\rho)}$ are the rotated stress and back stress defined in (3.16) and (3.17) where the $\Delta\omega_{ij}^{(\rho)}$ is given as

$$\Delta\omega_{ij}^{(\rho)} = \hat{\mathcal{A}}_{ijkl}^{(\rho)} (\Delta\bar{\epsilon}_{kl} + \Delta\bar{\omega}_{kl}) + \hat{a}_{ij}^{(\rho)} \Delta\theta \quad (4.29)$$

Note that the instantaneous concentration factors $\mathcal{A}_{ijkl}^{(\rho)}$, $\hat{\mathcal{A}}_{ijkl}^{(\rho)}$, $a_{ij}^{(\rho)}$ and $\hat{a}_{ij}^{(\rho)}$ computed from (4.19) to (4.22) depend on the instantaneous material properties (see (4.12)), which in turn depend on vector of plastic parameters $\Delta\lambda$ in $\Theta^{(m)}$, $\Delta\lambda \equiv [\Delta\lambda^{(1)}, \Delta\lambda^{(2)}, \dots, \Delta\lambda^{(n_y)}]^T$. Substituting (4.26) and (3.28) into the yield function (3.22) for each element in $\Theta^{(m)}$ yields a set of n nonlinear equations $\Phi \equiv [\Phi^{(1)}, \Phi^{(2)}, \dots, \Phi^{(n_y)}]^T$ with n_y unknown plastic parameters. The system of nonlinear equations is solved by the Newton method:

$$\Delta\lambda_{k+1}^{(\rho)} = \Delta\lambda_k^{(\rho)} - \left\{ \frac{\partial\Phi^{(\rho)}}{\partial\Delta\lambda^{(\eta)}} \right\}^{-1} \Phi^{(\eta)} \Bigg|_{\Delta\lambda_k^{(\rho)}} \quad (4.30)$$

A typical term in the jacobian matrix is given as

$$\frac{\partial\Phi^{(\rho)}}{\partial\Delta\lambda^{(\eta)}} = \mathfrak{N}_{ij}^{(\rho)} \{ I_{ijmn} + \Delta\lambda^{(\rho)} \mathcal{Q}_{ijmn}^{(\rho)} \}^{-1} \chi_{mn}^{(\rho\eta)} - \frac{4\delta_{\rho\eta} \beta h \{ Y^{(\rho)} \}^2}{9 - 6\beta h \Delta\lambda^{(\rho)}} \quad (4.31)$$

where

$$\chi_{mn}^{(\rho\eta)} = \frac{\partial\mathfrak{Z}_{mn}^{(\rho)}}{\partial\Delta\lambda^{(\eta)}} - \delta_{\rho\eta} \mathcal{Q}_{mnpq}^{(\rho)} (\sigma_{pq}^{(\rho)} - \alpha_{pq}^{(\rho)}) \quad (4.32)$$

$$\frac{\partial\mathfrak{Z}_{mn}^{(\rho)}}{\partial\Delta\lambda^{(\eta)}} = \frac{\partial({}^t\hat{\sigma}_{mn}^{(\rho)} - {}^t\hat{\alpha}_{mn}^{(\rho)})}{\partial\Delta\lambda^{(\eta)}} - L_{mnpq}^{(\rho)} \left(\frac{\partial\mathcal{A}_{pqst}^{(\rho)}}{\partial\Delta\lambda^{(\eta)}} (\Delta\bar{\epsilon}_{st} + \Delta\bar{\omega}_{st}) + \frac{\partial a_{pq}^{(\rho)}}{\partial\Delta\lambda^{(\eta)}} \Delta\theta \right) \quad (4.33)$$

In equation (4.33) $\partial(\hat{\sigma}_{mn}^{(\rho)} - \hat{\alpha}_{mn}^{(\rho)})/\partial\Delta\lambda^{(\eta)}$ depends on the derivatives of $\mathcal{A}_{pqst}^{(\rho)}$ and $a_{pq}^{(\rho)}$ with respect to $\Delta\lambda^{(\eta)}$. Evaluation of these derivatives is not trivial and hence the following approximation is employed:

$$\mathcal{A}_{pqst}^{(\rho)} \approx {}^t\mathcal{A}_{pqst}^{(\rho)}, \quad a_{pq}^{(\rho)} \approx {}^t a_{pq}^{(\rho)} \quad (4.34)$$

resulting in the block diagonal approximation of the jacobian matrix

$$\frac{\partial\Phi^{(\rho)}}{\partial\Delta\lambda^{(\eta)}} \approx -\delta_{\rho\eta} \left(\mathbf{n}_{ij}^{(\rho)} \hat{\chi}_{ij}^{(\rho)} + \frac{4\beta h \{Y^{(\rho)}\}^2}{9 - 6\beta h \Delta\lambda^{(\rho)}} \right) \quad (4.35)$$

where

$$\hat{\chi}_{ij}^{(\rho)} = (I_{ijmn} + \Delta\lambda^{(\rho)} \underline{\mathcal{G}}_{ijmn}^{(\rho)})^{-1} \underline{\mathcal{G}}_{mnpq}^{(\rho)} (\sigma_{pq}^{(\rho)} - \alpha_{pq}^{(\rho)}) \quad (4.36)$$

At each modified Newton iteration step the residual vector Φ is evaluated and the instantaneous concentration factors are recomputed from (4.12). The iterative process proceeds until the residual norm $\|\Phi\|_2$ vanishes up to a certain tolerance. The updated stress, yield stress and back stress for elements in $\Theta^{(m)}$ are calculated from (4.25), (3.28) and (3.29), respectively. For elements in $\Theta^{(f)}$, stresses can be obtained using (4.25) with $\Delta\lambda^{(\rho)} \equiv 0$. Finally, the macroscopic stress follows from (2.58).

4.3 Consistent Linearization for Incremental Homogenization Scheme

The instantaneous consistent stiffness properties are derived from consistent linearization of the constitutive equations. For elements in $\Theta^{(m)}$, taking the material time derivative of (4.25) and (3.29), and making use of (B.11) yields:

$$\begin{aligned} \dot{\sigma}_{ij}^{(\rho)} = & {}^t\dot{\hat{\sigma}}_{ij}^{(\rho)} + L_{ijmn}^{(\rho)} \{ \dot{\mathcal{A}}_{mnkl}^{(\rho)} (\Delta\bar{\epsilon}_{kl} + \Delta\bar{\omega}_{kl}) + \mathcal{A}_{mnpq}^{(\rho)} M_{pqkl} v_{k, x_l}^0 \} \\ & + L_{ijmn}^{(\rho)} \{ \dot{a}_{mn}^{(\rho)} \Delta\theta + (a_{mn}^{(\rho)} - \xi_{mn}^{(\rho)}) \dot{\theta} - \mathbf{n}_{mn}^{(\rho)} \dot{\lambda}^{(\rho)} - P_{mnpq} (\dot{\sigma}_{pq}^{(\rho)} - \dot{\alpha}_{pq}^{(\rho)}) \Delta\lambda^{(\rho)} \} \end{aligned} \quad (4.37)$$

and

$$\dot{\alpha}_{ij}^{(\rho)} = {}^t \dot{\hat{\alpha}}_{ij}^{(\rho)} + \frac{2(1-\beta)h}{3} \{ \mathfrak{N}_{ij}^{(\rho)} \dot{\lambda}^{(\rho)} + P_{ijpq} (\dot{\sigma}_{pq}^{(\rho)} - \dot{\alpha}_{pq}^{(\rho)}) \Delta \lambda^{(\rho)} \} \quad (4.38)$$

Substituting (B.11) into (4.37), then subtracting (4.38) from the resulting equation yields

$$\begin{aligned} \dot{\sigma}_{ij}^{(\rho)} - \dot{\alpha}_{ij}^{(\rho)} &= {}^t \dot{\hat{\sigma}}_{ij}^{(\rho)} - {}^t \dot{\hat{\alpha}}_{ij}^{(\rho)} + L_{ijmn}^{(\rho)} \{ \mathcal{A}_{mnpq}^{(\rho)} M_{pqkl} v_{k, x_l}^0 + (a_{mn}^{(\rho)} - \xi_{mn}^{(\rho)}) \dot{\theta} \} \\ &\quad - \varrho_{ijmn}^{(\rho)} \{ (\sigma_{mn}^{(\rho)} - \alpha_{mn}^{(\rho)}) \dot{\lambda}^{(\rho)} + (\dot{\sigma}_{mn}^{(\rho)} - \dot{\alpha}_{mn}^{(\rho)}) \Delta \lambda^{(\rho)} \} \end{aligned} \quad (4.39)$$

where in analogy to (4.34), we approximate $\dot{\mathcal{A}}_{mnhkl}^{(\rho)} = 0$ and $\dot{a}_{mn}^{(\rho)} = 0$.

From equations (A.8), (A.9) and (B.11) it follows that

$${}^t \dot{\hat{\sigma}}_{ij}^{(\rho)} = {}_{\sigma} U_{ijmn}^{(\rho)} (\hat{\mathcal{A}}_{mnhst}^{(\rho)} M_{stkl} v_{k, x_l}^0 + \hat{a}_{mn}^{(\rho)} \dot{\theta}) \quad (4.40)$$

$${}^t \dot{\hat{\alpha}}_{ij}^{(\rho)} = {}_{\alpha} U_{ijmn}^{(\rho)} (\hat{\mathcal{A}}_{mnhst}^{(\rho)} M_{stkl} v_{k, x_l}^0 + \hat{a}_{mn}^{(\rho)} \dot{\theta}) \quad (4.41)$$

Substituting (4.40) and (4.41) into (4.39) and collecting terms of $\dot{\sigma}_{ij}^{(\rho)} - \dot{\alpha}_{ij}^{(\rho)}$ gives

$$\dot{\sigma}_{ij}^{(\rho)} - \dot{\alpha}_{ij}^{(\rho)} = (I_{ijkl} + \Delta \lambda^{(\rho)} \varrho_{ijkl}^{(\rho)})^{-1} ({}_{\nu} \Xi_{klst} v_{s, x_t}^0 + \theta \Xi_{kl} \dot{\theta} + \lambda \Xi_{kl} \dot{\lambda}^{(m)}) \quad (4.42)$$

where

$${}_{\nu} \Xi_{klst} = \{ ({}_{\sigma} U_{klmn}^{(\rho)} - {}_{\alpha} U_{klmn}^{(\rho)}) \hat{\mathcal{A}}_{mnhuv}^{(\rho)} + L_{klmn}^{(\rho)} \mathcal{A}_{mnhuv}^{(\rho)} \} M_{uvst} \quad (4.43)$$

$$\theta \Xi_{kl} = ({}_{\sigma} U_{klmn}^{(\rho)} - {}_{\alpha} U_{klmn}^{(\rho)}) \hat{a}_{mn}^{(\rho)} + L_{klmn}^{(\rho)} (a_{mn}^{(\rho)} - \xi_{mn}^{(\rho)}) \quad (4.44)$$

$$\lambda \Xi_{kl} = -\varrho_{klmn}^{(\rho)} (\sigma_{mn}^{(m)} - \alpha_{mn}^{(m)}) \quad (4.45)$$

The value $\dot{\lambda}^{(\rho)}$ can be computed from the linearization of consistency conditions (see also Chapter 3.3) which yields

$$\dot{\lambda}^{(\rho)} = \Upsilon_{kl}^{(\rho)} ({}_{\nu} \Xi_{klst} v_{s, x_t}^0 + \theta \Xi_{kl} \dot{\theta}) \quad (4.46)$$

where

$$\Upsilon_{kl}^{(\rho)} = \frac{(9 - 6\beta h \Delta \lambda^{(\rho)}) \mathfrak{K}_{ij}^{(\rho)} (I_{ijkl} + \Delta \lambda^{(\rho)} \mathcal{Q}_{ijkl}^{(\rho)})^{-1}}{4\beta h \{Y^{(\rho)}\}^2 - (9 - 6\beta h \Delta \lambda^{(\rho)}) \mathfrak{K}_{mn}^{(\rho)} (I_{mnst} + \Delta \lambda^{(\rho)} \mathcal{Q}_{mnst}^{(\rho)})^{-1} \lambda \Xi_{st}} \quad (4.47)$$

and then substituting (4.46) into (4.42) yields

$$\dot{\sigma}_{ij}^{(\rho)} - \dot{\alpha}_{ij}^{(\rho)} = {}_v \Xi_{ijkl} v_{k, x_l}^0 + \theta \Xi_{ij} \dot{\theta} \quad (4.48)$$

where ${}_v \Xi_{ijkl}$ and $\theta \Xi_{ij}$ have identical structure to ${}_v \mathcal{S}_{ijkl}$ and $\theta \mathcal{S}_{ij}$ in (3.52) and (3.53) except that the symbols \mathcal{S} are replaced by Ξ , and $\Gamma^{(m)}$ by $\Upsilon^{(\rho)}$.

Substituting (4.46), (4.48) into (4.37) yields

$$\dot{\sigma}_{ij}^{(\rho)} = \mathcal{D}_{ijkl}^{(\rho)} v_{k, x_l}^0 + d_{ij}^{(\rho)} \dot{\theta} \quad \text{for} \quad \rho \in \Theta^{(m)} \quad (4.49)$$

where

$$\begin{aligned} \mathcal{D}_{ijkl}^{(\rho)} = & \sigma U_{ijmn}^{(\rho)} \hat{\mathcal{A}}_{mnst}^{(\rho)} M_{stkl} + L_{ijmn}^{(\rho)} \mathcal{A}_{mnpq}^{(\rho)} M_{pqkl} \\ & - L_{ijmn}^{(\rho)} (\mathfrak{K}_{mn}^{(\rho)} \Upsilon_{pq}^{(\rho)} {}_v \Xi_{pqkl} + \Delta \lambda^{(\rho)} P_{mnpq} {}_v \Xi_{pqkl}) \end{aligned} \quad (4.50)$$

and

$$d_{ij}^{(\rho)} = \sigma U_{ijmn}^{(\rho)} \hat{a}_{mn}^{(\rho)} + L_{ijmn}^{(\rho)} \{ (a_{mn}^{(\rho)} - \xi_{mn}^{(\rho)}) - \mathfrak{K}_{mn}^{(\rho)} \Upsilon_{pq}^{(\rho)} \theta \Xi_{pq} - \Delta \lambda^{(\rho)} P_{mnpq} \theta \Xi_{pq} \} \quad (4.51)$$

Similarly, the stress rate for elements in $\Theta^{(f)}$ is given by

$$\dot{\sigma}_{ij}^{(\eta)} = \mathcal{D}_{ijkl}^{(\eta)} v_{k, x_l}^0 + d_{ij}^{(\eta)} \dot{\theta} \quad \text{for} \quad \eta \in \Theta^{(f)} \quad (4.52)$$

where

$$\mathcal{D}_{ijkl}^{(\eta)} = \sigma U_{ijmn}^{(\eta)} \hat{\mathcal{A}}_{mnst}^{(\eta)} M_{stkl} + L_{ijmn}^{(\eta)} \mathcal{A}_{mnpq}^{(\eta)} M_{pqkl} \quad (4.53)$$

and

$$d_{ij}^{(\eta)} = \sigma U_{ijmn}^{(\eta)} \hat{a}_{mn}^{(\eta)} + L_{ijmn}^{(\eta)} (a_{mn}^{(\eta)} - \xi_{mn}^{(\eta)}) \quad (4.54)$$

The overall instantaneous stiffness \mathcal{D}_{ijkl} is obtained from the rate form of (2.64), equations (4.50), (4.51), (4.53) and (4.54):

$$\dot{\bar{\sigma}}_{ij} = \mathcal{D}_{ijkl} v_{k, x_l}^0 + d_{ij} \dot{\theta} \quad (4.55)$$

where

$$\mathcal{D}_{ijkl} = \sum_{\eta=1}^n c^{(\eta)} \mathcal{D}_{ijkl}^{(\eta)}, \quad \text{and} \quad d_{ij} = \sum_{\eta=1}^n c^{(\eta)} d_{ij}^{(\eta)} \quad (4.56)$$

$c^{(\eta)}$ denotes the ratio between the volume of element η and the volume of the unit cell at time $t + \Delta t$.

Finally, linearization of internal force vector yields:

$$\frac{d}{dt} f_A^{int} = \int_{\Omega} N_{iA, x_j} \bar{\mathcal{D}}_{ijkl} N_{kB, x_l} d\Omega \dot{q}_B + \int_{\Omega} N_{iA, x_j} d_{ij} \dot{\theta} d\Omega \quad (4.57)$$

$$\bar{\mathcal{D}}_{ijkl} = \mathcal{D}_{ijkl} + \delta_{kl} \bar{\sigma}_{ij} - \delta_{kj} \bar{\sigma}_{il} \quad (4.58)$$

where the first integral in (4.57) represents the consistent macroscopic tangent stiffness matrix for the n -point scheme model.

Remark (4): Approximating the piecewise constant phase rotations by a constant field in the entire unit cell domain as in Remark (3), (4.43) and (4.44) can be simplified as

$${}_v \Xi_{klst} = L_{klmn}^{(\rho)} \mathcal{A}_{mnuv}^{(\rho)} M_{uvst} - \{ \delta_{kn} (\sigma_{ml}^{(\rho)} - \alpha_{ml}^{(\rho)}) + \delta_{ln} (\sigma_{km}^{(\rho)} - \alpha_{km}^{(\rho)}) \} M_{[mn]st} \quad (4.59)$$

$${}_{\theta} \Xi_{kl} = L_{klmn}^{(\rho)} (a_{mn}^{(\rho)} - \xi_{mn}^{(\rho)}) \quad (4.60)$$

where (3.65) has been used. For elements in $\Theta^{(m)}$ (4.50) and (4.51) can be written as

$$\begin{aligned} \mathcal{D}_{ijkl}^{(\rho)} = & L_{ijmn}^{(\rho)} \mathcal{A}_{mnpq}^{(\rho)} M_{pqkl} - \{ \delta_{kn} (\sigma_{ml}^{(\rho)} - \alpha_{ml}^{(\rho)}) + \delta_{ln} (\sigma_{km}^{(\rho)} - \alpha_{km}^{(\rho)}) \} M_{[mn]st} \\ & - L_{ijmn}^{(\rho)} (\mathfrak{N}_{mn}^{(\rho)} \Upsilon_{pq}^{(\rho)} v_{pqkl} \Xi_{pqkl} + \Delta \lambda^{(\rho)} P_{mnpq} v_{pqkl} \Xi_{pqkl}) \end{aligned} \quad (4.61)$$

and

$$d_{ij}^{(\rho)} = L_{ijmn}^{(\rho)} \{ (a_{mn}^{(\rho)} - \xi_{mn}^{(\rho)}) - \kappa_{mn}^{(\rho)} \Upsilon_{pq}^{(\rho)} \Xi_{pq} - \Delta \lambda^{(\rho)} P_{mnpq} \bar{\Xi}_{pq} \} \quad (4.62)$$

On the other hand, for elements in $\Theta^{(f)}$ (4.53) and (4.54) are given by

$$\mathcal{D}_{ijkl}^{(\eta)} = L_{ijmn}^{(\eta)} \mathcal{A}_{mnpq}^{(\eta)} M_{pqkl} - (\delta_{in} \sigma_{mj}^{(\eta)} + \delta_{jn} \sigma_{im}^{(\eta)}) M_{[mn]kl} \quad (4.63)$$

and

$$d_{ij}^{(\eta)} = L_{ijmn}^{(\eta)} (a_{mn}^{(\eta)} - \xi_{mn}^{(\eta)}) \quad (4.64)$$

CHAPTER 5

ADAPTIVE MODEL CONSTRUCTION

In Chapters 3 and 4 we presented two schemes for modeling inelastic behavior of composite structures: the 2-point scheme and the n -point scheme. In the n -point scheme we employed a piecewise constant approximation of the eigenstrain field, whereas in the 2-point scheme the eigenstrain field and the elastic concentration factors in each phase are approximated by a constant. For the Nozzle Flap problem considered in [15] (see also Figure 1.1) the 2-point scheme is over three orders of magnitude faster than the n -point scheme. For linear problems the 2-point scheme with post-processing [8][11][15][16][19][20] is identical to the n -point scheme, whereas for nonlinear problems there is no such guarantee [42].

If we assume that the n -point and the 2-point schemes are optimal in terms of accuracy and speed, respectively, then it is natural to attempt to merge the two in a single model. In such a hybrid model, the 2-point scheme should be only used in regions where the modeling errors are small, whereas elsewhere the n -point scheme should be employed. We will refer to such a hybrid modeling strategy as the adaptive 2/ n -point scheme.

5.1 Modeling Error Estimation

The modeling error e^{2-pt} associated with the 2-point scheme can be defined as follows

$$e^{2-pt} = \left\| v^{ex} - v^{2-pt} \right\|_{\square} \quad (5.1)$$

where $\square = \Omega \times \Theta$ and

$$\|f\|_{\square}^2 = \frac{1}{\Theta} \int_{\Theta} \int_{\Omega} f^2 d\Theta d\Omega \quad (5.2)$$

v is an appropriate solution measure; the superscript ex refers to the exact solution within the framework of the mathematical homogenization theory, i.e., assuming solution periodicity. For estimation of errors resulting from lack of periodicity we refer to [16][38].

The key questions are: (i) how to estimate v^{ex} , (ii) what is a suitable measure for v , (iii) how to make the process of error estimation efficient, and (iv) how to utilize the model error estimation for adaptive construction of the $2/n$ -point model.

It is appropriate to recall that as the number elements in the unit cell is increased the solution obtained from the n -point scheme, denoted as v^{n-pt} , approaches the exact solution, i.e.,

$\lim_{n \rightarrow \infty} v^{n-pt} \rightarrow v^{ex}$. Even though the rate of convergence may not be monotonic, it is reasonable to

assume that for sufficiently large n the modeling error associated with the 2-point scheme can be approximated as

$$e^{2-pt} \approx E^{2-pt} = \|v^{n-pt} - v^{2-pt}\|_{\square} \quad (5.3)$$

We now turn to the second issue: the choice of v . In this context it is essential to interpret the 2-point scheme approach as consisting of two steps: analysis on the macroscale and post-processing on the microscale. In the first step, a nonlinear macro-analysis is carried out using the finite element method which utilizes the 2-point scheme. Consequently, the macroscopic deformation history is stored in a database at macro-Gauss points. In the post-processing step, the deformation field in a unit cell corresponding to critical macro-points is extracted from the database, and then subjected onto the unit cell as an external loading. Finally, the n -point scheme is employed to solve for selected unit cell problems.

Based on the above interpretation of the 2-point scheme, it follows that if the macroscopic deformation field obtained with the 2-point scheme is identical to one obtained with the n -point scheme, then the model error estimator, E^{2-pt} , should indicate zero error. In other words, v should be a measure of the macroscopic deformation field, whereas $\square = \Omega$. Possible deformation measures are: the macroscopic deformation gradient tensor, \mathbf{F} (the component form is defined in (3.61)), and/or incremental deformation measures represented by a pair $\Delta\bar{\mathbf{E}}, \Delta\bar{\mathbf{\Omega}}$. The former accounts for accumulation of errors

$$E_F^{2-pt} = \|\mathbf{F}^{n-pt} - \mathbf{F}^{2-pt}\|_{\Omega} \quad (5.4)$$

whereas the latter controls the incremental errors

$$E_{\Delta}^{2-pt} = \sqrt{\|\Delta\bar{\epsilon}^{n-pt} - \Delta\bar{\epsilon}^{2-pt}\|_{\Omega}^2 + \|\Delta\bar{\omega}^{n-pt} - \Delta\bar{\omega}^{2-pt}\|_{\Omega}^2} \quad (5.5)$$

In Chapter 6 we will show that in a confined deformation pattern, where small plastic zones are encompassed by elastically deforming solid, the modeling errors, E^{2-pt} , are very small, whereas in large plastic zones dominated by matrix deformation, the modeling errors, E^{2-pt} , might be significant. For simplicity, we adopt the incremental estimator (5.5).

We now turn to the computational efficiency issue. Estimation of modeling error based on equations (5.4) and (5.5) necessitates solution of the n -point scheme model. As indicated earlier the computational cost of the n -point scheme model is enormous, and hence, only an estimate of E^{2-pt} , denoted \underline{E}^{2-pt} , will be evaluated. The philosophy behind our modeling error estimator is somewhat similar to that employed for estimation of discretization errors, namely, if the mathematical model (or discretization) is locally altered, then in absence of the pollution errors the solution outside the local region is not significantly affected, and thus the bulk of the error can be computed on the local level. This process avoids the need for solving an auxiliary global problem and replaces it by solving a sequence of problems on small local domains.

When the aforementioned procedure is applied for estimation of discretization errors, the computational cost of solving the local problem is relatively low, reducing the cost of discretization error estimation to one of a manageable size. Unfortunately, this is not the case for estimation of modeling error \underline{E}^{2-pt} . Even though the aforementioned process involves multiple solutions of small local problems (for example, on the macro-element domains), the cost of applying the n -point scheme on each macro-element is formidable in a large scale computational environment. Therefore, the costly n -point scheme should be utilized only for those macro-elements which have been identified as “having potential to be critical” by some simple cost-effective engineering-based criteria. One possible engineering criterion is the magnitude of the deformation, measured by a norm of one of the macroscopic strain measures. When this norm exceeds some critical value, the corresponding macro element is tagged for *a-posteriori* model error estimation.

5.2 Adaptive 2/ n -Point Scheme

We now focus on the adaptive 2/ n -point model construction. Consider the 2/ n -point model at time t , consisting of the 2-point scheme model in the portion of the macro-domain ${}^t\Omega^{2-pt} \subset {}^t\Omega$ and

the n -point scheme model in the remainder ${}^t\Omega^{n-pt}$ such that ${}^t\Omega^{2-pt} \cup {}^t\Omega^{n-pt} = {}^t\Omega$. The goal is to adaptively construct the $2/n$ -point model at time $t + \Delta t$, consisting of subdomains ${}^{t+\Delta t}\Omega^{2-pt}$ and ${}^{t+\Delta t}\Omega^{n-pt}$. Let ${}^t_{cr}\Omega^{2-pt} = \bigcup_e {}^t_{cr}\Omega_e^{2-pt}$ be a subdomain in ${}^t\Omega^{2-pt}$ consisting of ${}_{cr}n$ macro-element subdomains ${}^t_{cr}\Omega_e^{2-pt}$ which have been tagged as critical by the aforementioned engineering criterion, as shown in Figure 5.1.

Let ${}^\tau_{cr}\Delta\bar{\epsilon}_e^{2-pt}$ and ${}^\tau_{cr}\Delta\bar{\omega}_e^{2-pt}$ be the macro-strain and rotation increments on ${}^\tau_{cr}\Omega_e^{2-pt}$ at $\tau \leq t$. The first step in the adaptive process is to post-process the unit cell solution at time t for all macro-elements on ${}^t_{cr}\Omega_e^{2-pt}$ by utilizing the n -point scheme model outlined in Chapter 4.

Let ${}_{cr}\mathbf{r}_e^{2-pt}$ be the residual for all the elements on ${}^t_{cr}\Omega_e^{2-pt}$ defined as

$${}_{cr}\mathbf{r}_e^{2-pt} = {}^{t+\Delta t}_{cr}\mathbf{f}_e^{2-pt} - {}^t_{cr}\mathbf{f}_e^{2-pt} \quad (5.6)$$

where ${}^t_{cr}\mathbf{f}_e^{2-pt}$ is the corresponding internal force vector. In the second step, for all elements in ${}^t_{cr}\Omega_e^{2-pt}$ the incremental nonlinear problem defined as

$${}_{cr}\mathbf{r}_e^{2-pt} = \mathbf{0} \quad (5.7)$$

is solved twice: first, by using the 2-point scheme model, and second, by utilizing the n -point scheme model with initial conditions obtained via post-processing. The estimated error on ${}^t_{cr}\Omega_e^{2-pt}$ is computed by utilizing equation (5.5)

$$E_{\Delta t}^{2-pt} = \sqrt{\left\| {}_{cr}\Delta\bar{\epsilon}_e^{n-pt} - {}_{cr}\Delta\bar{\epsilon}_e^{2-pt} \right\|_{{}^t_{cr}\Omega_e^{2-pt}}^2 + \left\| {}_{cr}\Delta\bar{\omega}_e^{n-pt} - {}_{cr}\Delta\bar{\omega}_e^{2-pt} \right\|_{{}^t_{cr}\Omega_e^{2-pt}}^2} \quad (5.8)$$

where the strain and rotation increments are evaluated by solving equation (5.7).

The total modeling error is then estimated as

$$E_{\Delta}^{2-pt} \approx \sqrt{\sum_{e \in {}^t\Omega_e^{2-pt}} \frac{c_r^n}{c_r^n} (E_{\Delta_e}^{2-pt})^2} \quad (5.9)$$

To steer the process of adaptivity we define the modeling error indicator η_{Δ_e} on ${}^t\Omega_e^{2-pt}$ as

$$\eta_{\Delta_e} = \frac{E_{\Delta_e}^{2-pt}}{\Delta p_{av}} \quad (5.10)$$

where

$$p_{\Delta}^{av} = \sqrt{\frac{\|\Delta \bar{\varepsilon}^{2-pt} + \Delta \bar{\omega}^{2-pt}\|_{c_r \Omega_e^{2-pt}}^2 + (E_{\Delta}^{2-pt})^2}{c_r^n}} \quad (5.11)$$

p_{Δ}^{av} represents the average incremental deformation in a single element located in ${}^t\Omega_e^{2-pt}$. We replace the 2-point scheme model by the n -point scheme model for all the elements on ${}^t\Omega_e^{2-pt}$ for which $\eta_{\Delta_e} \geq tol$. A typical value for tol is between 1% to 10% depends on the accuracy requirement.

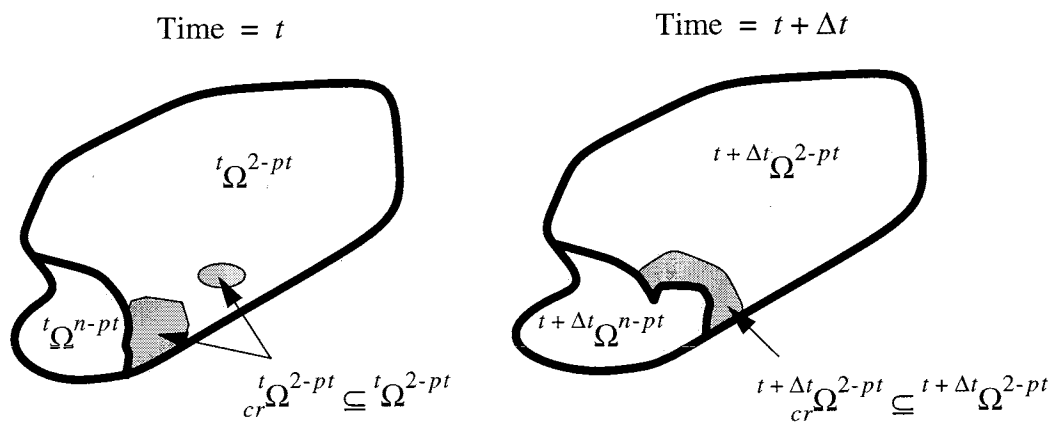


Figure 5.1 Adaptive model construction

CHAPTER 6

NUMERICAL EXPERIMENTS

Our numerical experimentation agenda consists of three examples. The first is used to validate our finite deformation plasticity formulation. The second and the third examples test the proposed adaptive $2/n$ -point scheme in a deformation pattern with large plastic zones dominated by matrix deformation as well as in a typical confined deformation pattern, where a small plastic zone is encompassed by an elastically deforming solid.

6.1 Uniform Macro-Strain Loading

The objective of the first example is to carry out a qualitative assessment of the large deformation formulation. The primary “suspect” is equation (3.10) which decomposes displacement field in the microstructure into two parts: the macroscopic part which comes from the integration of the non-periodic macroscopic strain and rotation increments (the first term in (3.10)) and the periodic microscopic part (the second term in (3.10)). Note that solution update in the unit cell domain directly from the asymptotic expansion of the displacement field (2.11) is not feasible, because in the limit as $\zeta \rightarrow 0$, only the macroscopic part has contribution. On the other hand, if \mathbf{u}^1 is considered only, then the nonperiodic finite deformation patterns are not accounted for.

As a test problem we select a macro problem subjected to the state of uniform strain field (or linear displacement field). A unit cell consists of a stiff elastic cylindrical fiber embedded in a compliant plastically deforming matrix. The phase properties are given below:

Fiber: Young’s modulus = 68.9 GPa, Poisson’s ratio = 0.21

Matrix: Young’s modulus = 6.89 GPa, Poisson’s ratio = 0.33, yield stress = 24 MPa,
isotropic hardening modulus = 0.689 GPa, $\beta = 1$.

We consider a uniform transverse tension, transverse shear and longitudinal shear loading conditions. The overall principal Green strain does not exceed 25% in all three cases. Figures 6.1 to 6.3 show the contribution of macroscopic and microscopic fields to the total deformation field in the unit cell. It can be seen that each of the two contributing parts alone significantly distort the circular fiber cross section, but their sum recovers the original fiber shape, as expected in a matrix dominated loading condition.

6.2 The 3D Beam Problem

To validate the computational models and adaptive strategies proposed we comprise a test case, where a significant portion of the structure is subjected to the matrix dominated deformation in a load or stress control mode (as opposed to displacement control). This is the worse possible scenario in terms of accuracy for the 2-point scheme. The problem configuration is shown in Figure 6.4. The macro problem is discretized with 5635 tetrahedral finite elements. The microstructure is the same one used in the previous example. The fiber direction coincides with the beam's longitudinal direction. In the region of length l_1 from the fixed end the beam is subjected to the shear deformation (which is the matrix dominated mode) whereas in the remainder of the problem domain, l_2 length, the beam is in pure bending, which is a fiber dominated mode of loading. The phase properties are summarized below:

Fiber: Young's modulus = 37.92 GPa, Poisson's ratio = 0.21

Matrix: Young's modulus = 6.89 GPa, Poisson's ratio = 0.33, yield stress = 24 MPa,
isotropic hardening modulus = 0.689 GPa, $\beta = 1$.

The loading is applied in 15 load steps. The maximal vertical displacement at the free end is over one third of the length of the beam and the stresses exceed the elastic limit in all macro-elements.

The problem is solved using the 2-point scheme with micro-history recovery, the adaptive $2/n$ -point scheme, and the n -point scheme for a comparison purpose. Figure 6.5 shows the evolution of the normalized estimated local error in the vicinity of the fixed end as obtained with the 2-point scheme (equation (5.10)). It can be seen that the maximal normalized local error in the region dominated by matrix deformation is 40%. In a region dominated by the fiber deformation the error does not exceed 3%. The distribution of the local principal stress error in the critical unit cell (denoted by point A in Figure 6.5) as obtained with the 2-point scheme and micro-history postprocessing is shown in Figure 6.6. It can be seen that the normalized error in the unit cell is of the same magnitude as the normalized local error in the macrostructure. Figure 6.7 illustrates the evolution of the normalized local error in the macrostructure obtained using the adaptive $2/n$ -point scheme model. The maximal normalized local error is less than 1% and the normalized error in the unit cell follows the same trend as shown in Figure 6.8.

We conclude that the adaptive $2/n$ -point scheme model outperforms the 2-point scheme model in terms of accuracy (0.8% maximal error as compared to 40%), and the n -point scheme model in terms of CPU time as it is 14 times faster than the n -point scheme.

6.3 The Nozzle Flap Problem

For the final numerical example, we consider a typical aerospace component where only a small region experiences inelastic deformation. The finite element mesh describing the macrostructure of the Nozzle Flap is shown in Figure 1.1. We consider two types of microstructures: (i) the fibrous unit cell (as in the previous example) and the plain weave fabric microstructure shown in Figure 6.9. The fibrous unit cell contains 98 elements in the fiber domain and 253 elements in the matrix domain. The fiber volume fraction is 0.27. The plain weave microstructure has 370 elements in the fiber bundle and 1196 in the matrix domain. The bundle volume fraction is 0.25. The phase properties are:

Fiber, fiber bundle:	Young's modulus = 379.2 GPa, Poisson's ratio = 0.21
Matrix:	Young's modulus = 68.9 GPa, Poisson's ratio = 0.33, yield stress = 24 MPa, isotropic hardening = 14 GPa, $\beta = 1$.

The Nozzle Flap is subjected to an aerodynamic force (simulated by a uniform pressure) on the back of the flap. We assume that the pin-eyes are rigid and a rotation is not allowed so that all the degrees of freedom on the pin-eye surfaces are fixed. The loading takes the solution well into the inelastic region in the vicinity of the pins: 15% of elements experience inelastic deformation in the case of fibrous microstructure, and 29% in the case of plain weave.

- The problem is analyzed using the adaptive $2/n$ -point scheme model. Figure 6.10 shows that the 2-point scheme model yields the maximum normalized local error in the macrostructure below 1% (for the plain weave microstructure). Hence, if the tolerance for switching from the 2-point scheme to the n -point scheme is higher than 1%, adaptive strategy selects the 2-point scheme model in the entire macro problem domain. The normalized local error in the unit cell located at Point C of Figure 6.10 is 2.5% for fibrous microstructure and 6.5% for the plain weave, as shown in Figures 6.11 and 6.12.

For the problem with the fibrous unit cell, the CPU time on a SPARC 10/51 is 30 seconds for the macroscopic analysis and 120 seconds for postprocessing a single point. For the plain weave microstructure, the macroscopic analysis consumes 30 seconds, whereas postprocessing takes 510 seconds per point. On the other hand, the n -point scheme consumes 7 hours of CPU time for fibrous composite and over 55 hours of CPU time for plain weave. Memory requirement ratios are approximately 1:250 for the fibrous unit cell and 1:1200 for the plain weave in favor of the $2/n$ -point scheme (or 2-point scheme).

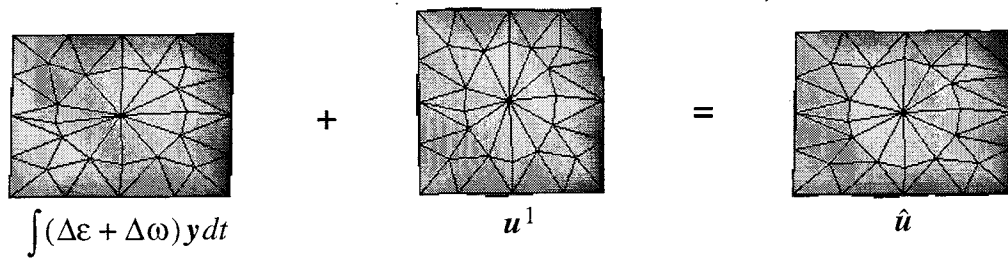


Figure 6.1 Deformation of unit cell under transverse tension

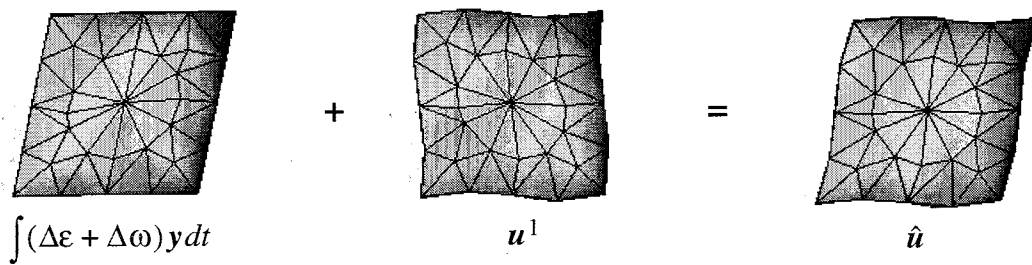


Figure 6.2 Deformation of unit cell under transverse shear

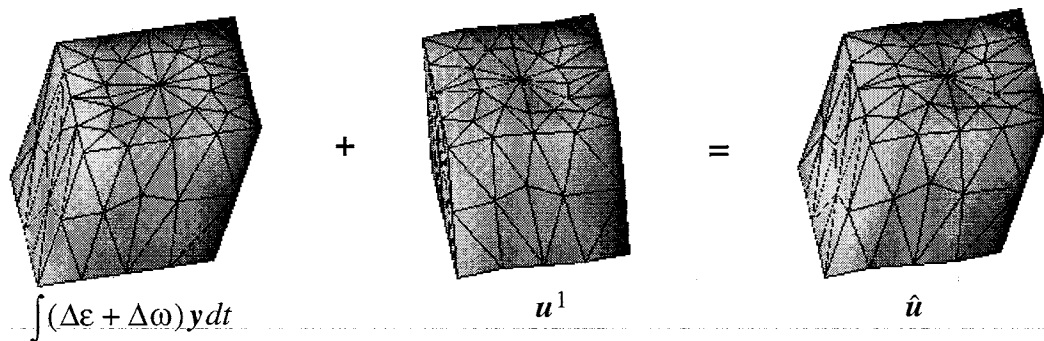


Figure 6.3 Deformation of unit cell under longitudinal shear

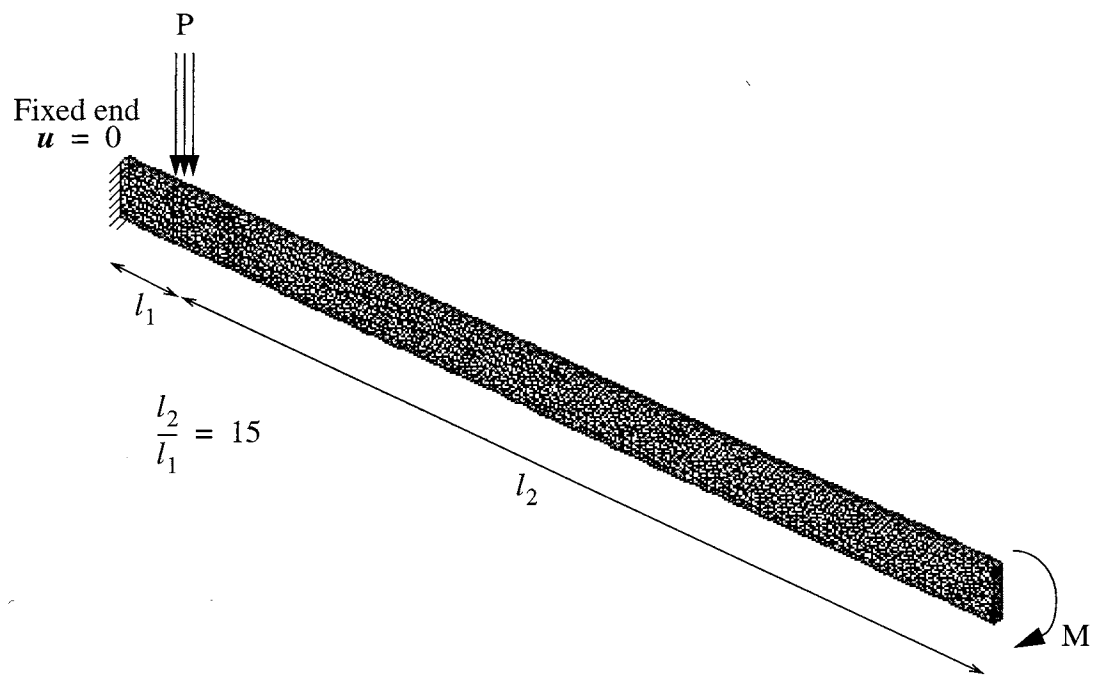


Figure 6.4 Finite element mesh for the 3D beam problem

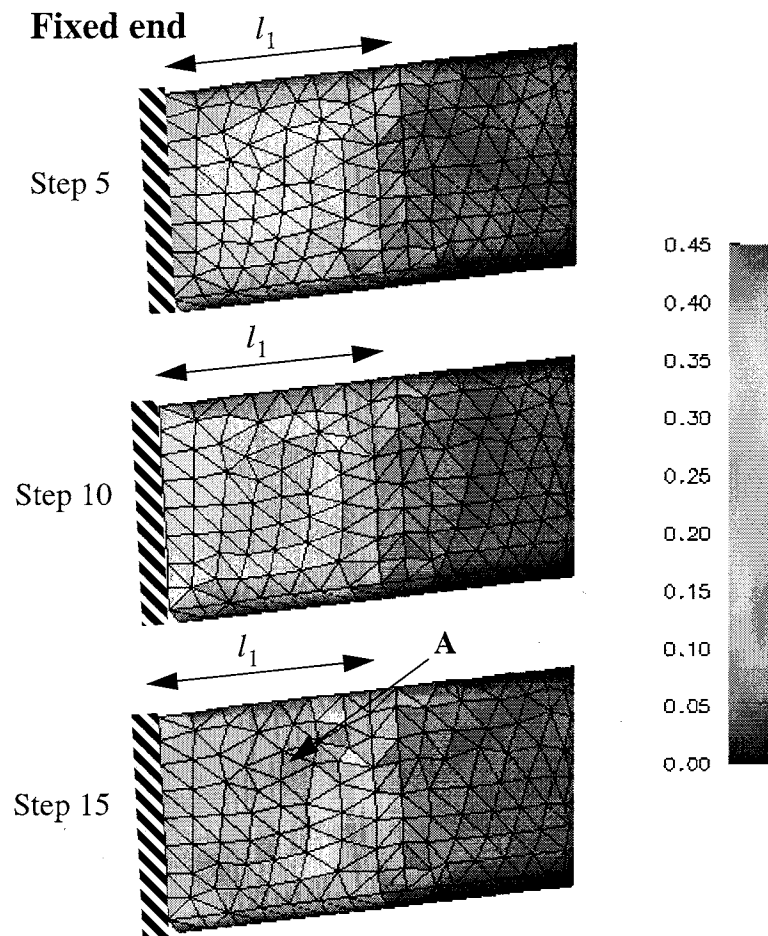


Figure 6.5 Distribution of the normalized local error with the 2-point model

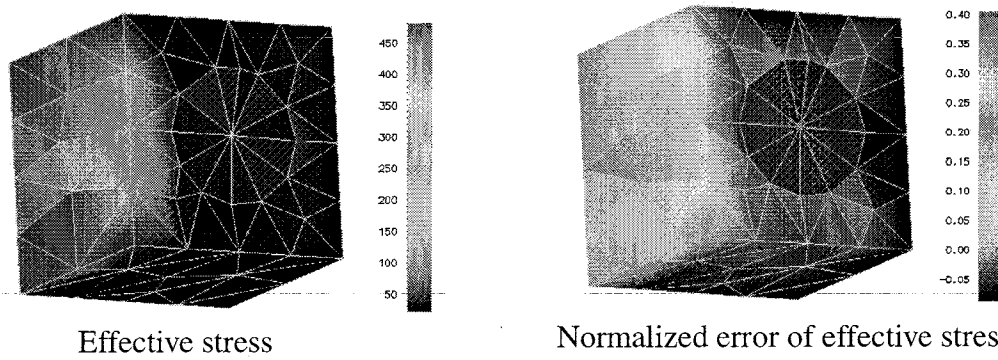


Figure 6.6 Effective stress and normalized error at point A with the 2-point model

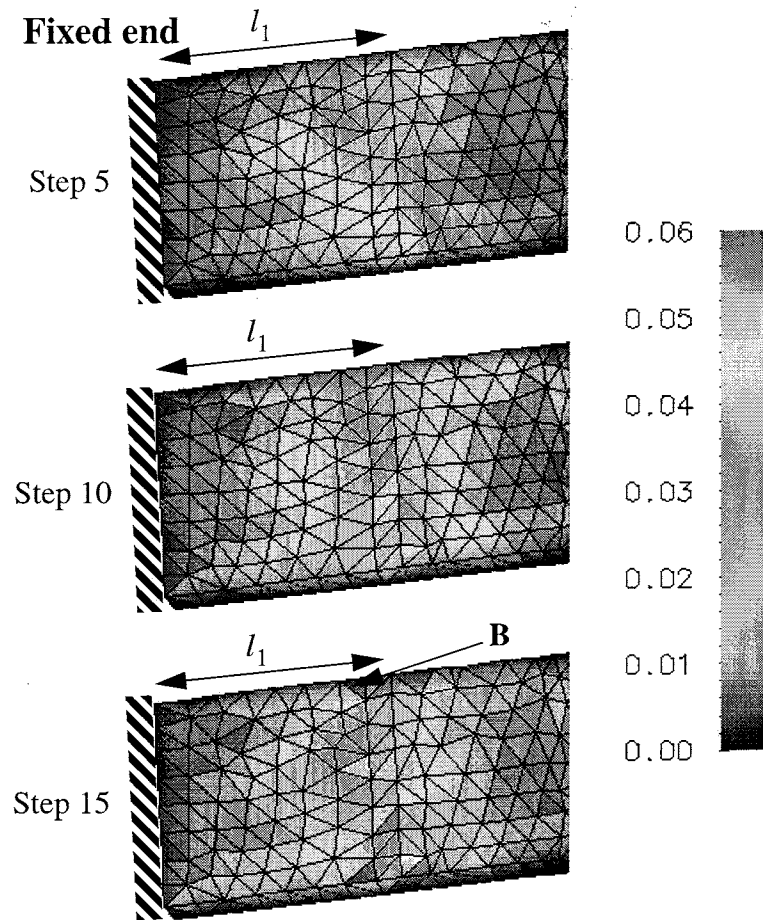


Figure 6.7 Distribution of the normalized local error with the $2/n$ -point model

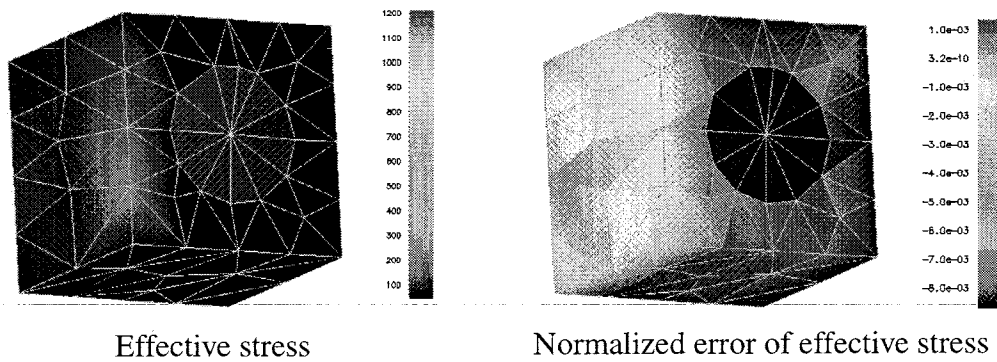


Figure 6.8 Effective stress and normalized error at point B with the $2/n$ -point model

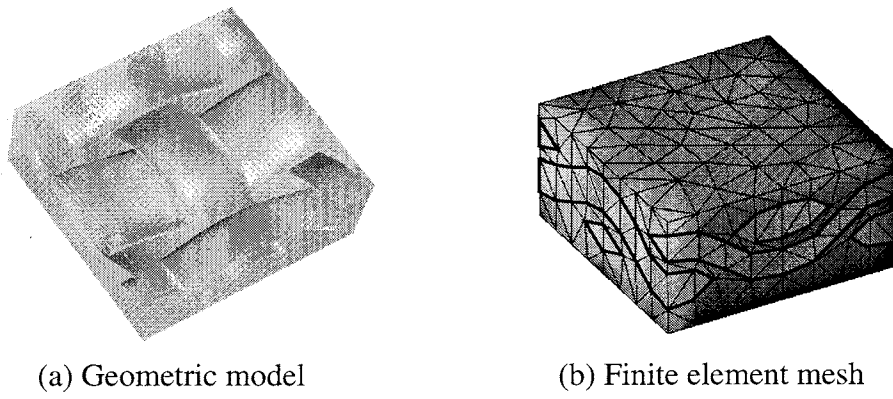


Figure 6.9 Geometric model and FE mesh of the plain weave unit cell

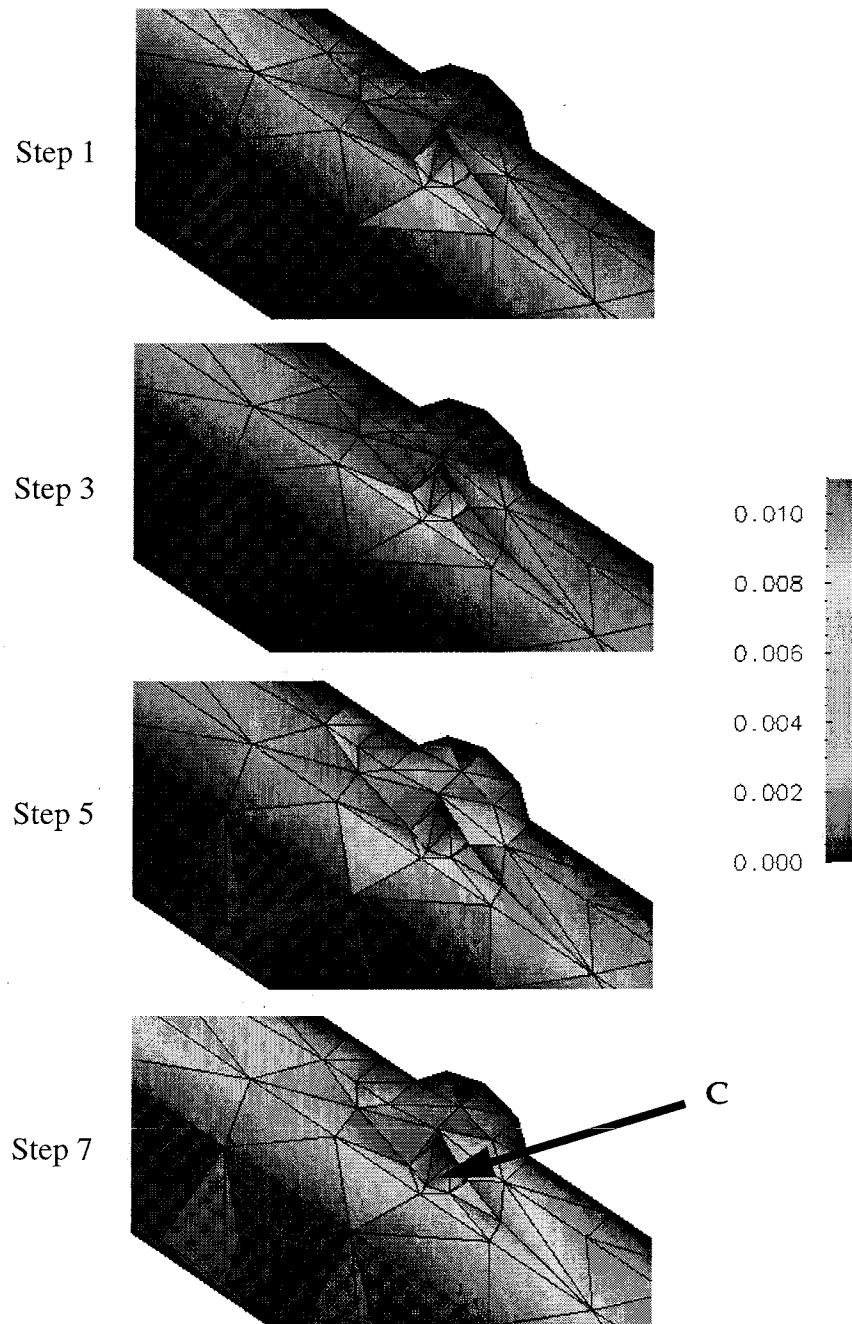


Figure 6.10 Distribution of the normalized local error in the nozzle flap with plain weave unit cell

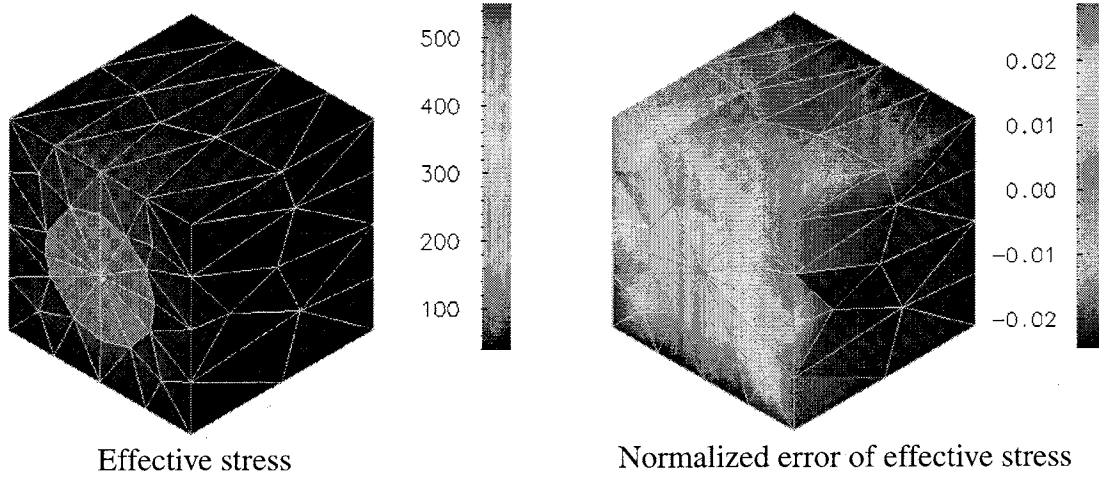


Figure 6.11 Effective stress and normalized error for fibrous unit cell

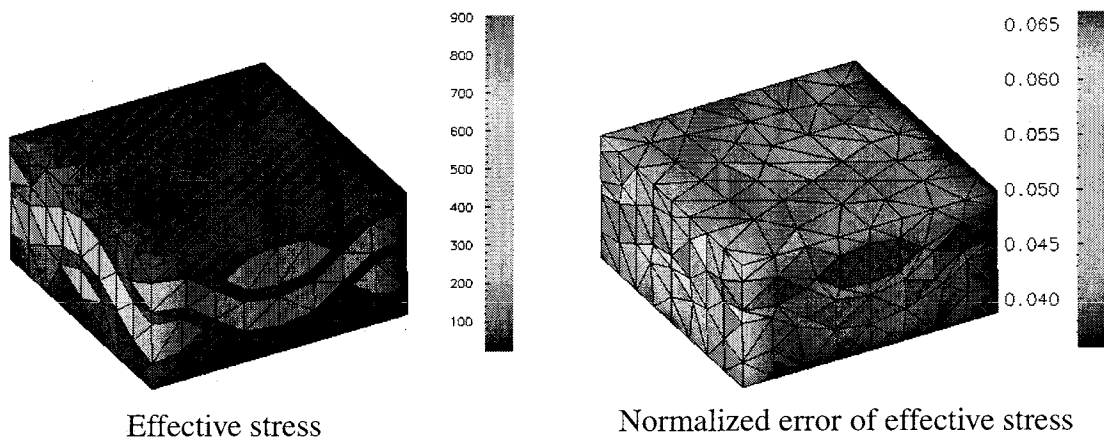


Figure 6.12 Effective stress and normalized error for plain weave unit cell

CHAPTER 7

CONCLUSIONS AND FUTURE RESEARCH DIRECTIONS

An alternative to the classical mathematical homogenization theory for finite deformation plasticity problems, which provides a comparable accuracy to the classical theory but at a fraction of computational cost, has been developed. For the numerical example considered, the speedup factor was several orders of magnitude as compared to the classical theory, whereas the maximum error in stresses was less than 3% (Chapter 6.3).

The present work by no means represents a complete account of all theoretical and numerical issues related to inelastic analysis of heterogeneous media. First, the present theory is no more accurate than the classical mathematical homogenization theory, but provides a comparable accuracy at a greater speed. It is important to note that assumptions of periodicity and uniformity of macroscopic fields within a unit cell domain, which are embedded within the two theories, may yield inaccurate solutions in the vicinity of boundary layers or areas of high stress/strain concentration such as cracks or shear bands. The remedies to this phenomenon, ranging from changing the size of the unit cell to carrying out an iterative global-local analysis, have been recently reported in [38][49] for linear elastic problems. Secondly, various failure modes, other than matrix plasticity, such as delamination, debonding, or matrix cracking have not been accounted for in the present thesis. These aspects, together with issues of stability and uniqueness and multiple time scales in rate sensitive constitutive equations at the micromechanical and macromechanical levels, are among the topics of our future investigation.

REFERENCES

1. J. Aboudi, "A Continuum Theory for Fiber-Reinforced Elastic-Viscoplastic Composites," *International Journal of Engineering Science*, 20, 1982.
2. J. Aboudi, "Elastoplasticity Theory for Composite Materials," *Solid Mechanics Archives*, 11, 1986.
3. M. L. Accorsi and S. Nemat-Nasser, "Bounds on the Overall Elastic and Instantaneous Elastoplastic Moduli of Periodic Composites," *Mechanics of Materials*, 5, 1986.
4. A. Benssousan, J. L. Lions and G. Papanicoulau, *Asymptotic Analysis for Periodic Structure*, North-Holland, 1978.
5. N. S. Bakhvalov and G. P. Panasenko, *Homogenisation: Averaging Processes in Periodic Media*, Kluwer Academic Publishers, 1989.
6. G. J. Dvorak, "On Uniform Fields in Heterogeneous Media," *Proceedings Royal Society of London*, A431, 1990.
7. G. J. Dvorak, "Plasticity Theories for Fibrous Composite Materials," in R. K. Everett and R. J. Arsenault, editors, *Metal Matrix Composites: Mechanisms and Properties*, Academic Press, 1991.
8. G. J. Dvorak, "Transformation Field Analysis of Inelastic Composite Materials," *Proceedings Royal Society of London*, A437, 1992.
9. G. J. Dvorak and Y. A. Bahei-El-Din, "Plasticity Analysis of Fibrous Composites," *Journal of Applied Mechanics*, 49, 1982.
10. G. J. Dvorak and Y. A. Bahei-El-Din, "A Bimodal Plasticity Theory of Fibrous Composite Materials," *Acta Mechanica*, 69, 1987.
11. G. J. Dvorak, Y. A. Bahei-El-Din and A. M. Wafa, "Implementation of the Transformation Field Analysis for Inelastic Composite Materials," *Computational Mechanics*, 14, 1994.
12. G. J. Dvorak and M. S. M. Rao, "Axisymmetric Plasticity Theory of Fibrous Composites," *International Journal of Engineering Science*, 14, 1976.
13. N. Fares and G. J. Dvorak, "Large Elastic-Plastic Deformations of Fibrous Metal Matrix Composites," *Journal of the Mechanics and Physics of Solids*, 39, 1991.
14. J. Fish, P. Nayak and M. H. Holmes, "Microscale Reduction Error Indicators and Estimators for a Periodic Heterogeneous Medium," *Computational Mechanics*, 14, 1994.
15. J. Fish, K. Shek, M. Pandheeradi and M. S. Shephard, "Computational Plasticity for Composite Structures Based on Mathematical Homogenization: Theory and Practice," *Computer Methods in Applied Mechanics and Engineering*, accepted for

publication.

16. J. Fish and A. Wagiman, "Multiscale Finite Element Method for Locally Nonperiodic Heterogeneous Medium," *Computational Mechanics*, 12, 1993.
17. S. Ghosh and S. Moorthy, "Elastic-Plastic Analysis of Arbitrary Heterogeneous Materials with the Voronoi Cell Finite Element Method," *Computer Methods in Applied Mechanics and Engineering*, 121, 1995.
18. M. Gosz, B. Moran and J. D. Achenbach, "Matrix Cracking in Transversely Loaded Fiber Composites with Compliant Interphases," AMD-Vol. 150/AD-Vol. 32, *Damage Mechanics in Composites*, ASME, 1992.
19. J. M. Guedes, *Nonlinear Computational Models for Composite Materials Using Homogenization*, PhD thesis, University of Michigan, 1990.
20. J. M. Guedes and N. Kikuch, "Preprocessing and Postprocessing for Materials Based on the Homogenization Method with Adaptive Finite Element Methods," *Computer Methods in Applied Mechanics and Engineering*, 83, 1990.
21. J. O. Hallquist, *NIKE2D: An Implicit, Finite Deformation, Finite Element Code for Analyzing the Static and Dynamic Response of Two Dimensional Solids*, University of California, Lawrence Livermore National Laboratory, Report UCID-19156, 1979.
22. R. Hill, "A Theory of the Yielding and Plastic Flow of Anisotropic Metals," *Proceedings of Royal Society of London*, A193, 1948.
23. R. Hill, "A Self Consistent Mechanics of Composite Materials," *Journal of the Mechanics and Physics of Solids*, 13, 1965.
24. R. Hill, "The Essential Structure of Constitutive Laws for Metal Composites and Polycrystals," *Journal of the Mechanics and Physics of Solids*, 15, 1967.
25. T. J. R. Hughes, "Numerical Implementation of Constitutive Models: Rate-Independent Deviatoric Plasticity," in S. Nemat-Nasser, R. J. Asaro and G. A. Hegemier, editors, *Theoretical Foundation for Large Scale Computations for Nonlinear Material Behavior*, Martinus Nijhoff Publishers, 1983.
26. T. J. R. Hughes and J. Winget, "Finite Rotation Effects in Numerical Integration of Rate Constitutive Equations Arising in Large Deformation Analysis," *International Journal of Numerical Methods in Engineering*, 15, 1980.
27. S. Jansson, "Homogenized Nonlinear Constitutive Properties and Local Stress Concentrations for Composites with Periodic Internal Structure," *International Journal of Solids and Structures*, 29, 1992.
28. A. L. Kalamkarov, *Composite and Reinforced Elements of Construction*, John Wiley and Sons, 1992.
29. E. H. Lee, R. L. Mallett and T. B. Wertheimer, "Stress Analysis for Kinematic Hardening in Finite Deformation Plasticity," *Journal of Applied Mechanics*, 105, 1983.

30. F. Lene and D. Leguillon, "Homogenized Constitutive Law for a Partially Cohesive Composite Material," *International Journal of Solids and Structures*, 18, 1982.
31. F. Lene, "Damage Constitutive Relations for Composite Materials," *Engineering Fracture Mechanics*, 25, 1986.
32. V. M. Levin, "Thermal Expansion Coefficients of Heterogeneous Materials," *Mekhanika Tverdogo Tela*, 2, 1967.
33. T. H. Lin, D. Salinas and Y. M. Ito, "Effects of Hydrostatic Stress on the Yielding of Cold Rolled Metals and Fiber-Reinforced Composites," *Journal of Composite Materials*, 26, 1972.
34. C. J. Lissenden and C. T. Herakovich, "Numerical Modeling of Damage Development and Viscoplasticity in Metal Matrix Composites," *Computer Methods in Applied Mechanics and Engineering*, 126, 1995.
35. T. Mori and K. Tanaka, "Average Stress in Matrix and Average Elastic Energy of Materials with Misfitting Inclusions," *Acta Metallurgica*, 21, 1973.
36. H. Moulinec and P. Suquet, "A Fast Numerical Method for Computing the Linear and Nonlinear Properties of Composites," *C. R. Acad. Sc. Paris II*, 318, 1994.
37. S. Nemat-Nasser, "On Finite Plastic Flow of Crystalline and Geomaterials," *Journal of Applied Mechanics*, 105, 1983.
38. J. T. Oden and T. I. Zohdi, *Analysis and Adaptive Modeling of Highly Heterogeneous Elastic Structures*, TICAM Report 56, University of Texas at Austin, 1996.
39. P. Ponte Castaneda, "New Variational Principles in Plasticity and Their Applications to Composite Materials," *Journal of the Mechanics and Physics of Solids*, 40, 1992.
40. S. A. Rizzi, A. R. Leewood, J. F. Doyle and C. T. Sun, "Elastic-Plastic Analysis of Boron/Aluminium Composite under Constrained Plasticity Conditions," *Journal of Composite Materials*, 21, 1987.
41. E. Sanchez-Palencia and A. Zaoui, *Homogenization Techniques for Composite Media*, Springer-Verlag, 1987.
42. R. S. Shah, *Modeling and Analysis of High Temperature Inelastic Deformation in Metal Matrix Composites*, PhD thesis, Rensselaer Polytechnic Institute, 1991.
43. J. C. Simo and R. L. Taylor, "Consistent Tangent Operators for Rate-Independent Elastoplasticity," *Computer Methods in Applied Mechanics and Engineering*, 48, 1985.
44. P. M. Suquet, *Plasticite et Homogenisation*, These de Doctorat d'Etat, Universite Pierre et Marie Curie, Paris 6, 1982.
45. P. M. Suquet, "Elements of Homogenization for Inelastic Solid Mechanics," in E. Sanchez-Palencia and A. Zaoui, editors, *Homogenization Techniques for Composite Media*, Springer-Verlag, 1987.

46. J. L. Teply and G. J. Dvorak, "Bounds on Overall Instantaneous Properties of Elastic-Plastic Composites," *Journal of the Mechanics and Physics of Solids*, 36, 1988.
47. J. R. Willis, "On Methods for Bounding the Overall Properties of Nonlinear Composites," *Journal of the Mechanics and Physics of Solids*, 39, 1991.
48. H. Zielger, "A Modification of Prager's Hardening Rule," *Quarterly of Applied Mathematics*, 17, 1959.
49. T. I. Zohdi, J. T. Oden and G. J. Rodin, *Hierarchical Modeling of Heterogeneous Bodies*, TICAM Report 21, University of Texas at Austin, 1996.

APPENDIX A

DERIVATION OF $\partial(\sigma_{ij}^{(m)} - \alpha_{ij}^{(m)})/\partial\Delta\lambda^{(m)}$

Consider equation (3.34):

$$\sigma_{ij}^{(m)} - \alpha_{ij}^{(m)} = (I_{ijkl} + \Delta\lambda^{(m)} \wp_{ijkl})^{-1} ({}_{ir}\sigma_{kl}^{(m)} - {}^t\hat{\alpha}_{kl}^{(m)}) \quad (\text{A.1})$$

Taking derivative of (A.1) with respect to $\Delta\lambda^{(m)}$ yields:

$$\begin{aligned} \frac{\partial}{\partial\Delta\lambda^{(m)}}(\sigma_{ij}^{(m)} - \alpha_{ij}^{(m)}) &= (I_{ijkl} + \Delta\lambda^{(m)} \wp_{ijkl})^{-1} \\ &\quad \left(-\wp_{klmn}(\sigma_{mn}^{(m)} - \alpha_{mn}^{(m)}) + \frac{\partial}{\partial\Delta\lambda^{(m)}}({}_{ir}\sigma_{kl}^{(m)} - {}^t\hat{\alpha}_{kl}^{(m)}) \right) \end{aligned} \quad (\text{A.2})$$

where the last term can be written as

$$\frac{\partial({}_{ir}\sigma_{kl}^{(m)} - {}^t\hat{\alpha}_{kl}^{(m)})}{\partial\Delta\lambda^{(m)}} = \frac{\partial({}^t\hat{\sigma}_{kl}^{(m)} - {}^t\hat{\alpha}_{kl}^{(m)})}{\partial\Delta\lambda^{(m)}} = \frac{\partial({}^t\hat{\sigma}_{kl}^{(m)} - {}^t\hat{\alpha}_{kl}^{(m)})}{\partial\Delta\omega_{pq}^{(m)}} \frac{\partial\Delta\omega_{pq}^{(m)}}{\partial\Delta\lambda^{(m)}} \quad (\text{A.3})$$

and

$$\begin{aligned} \frac{\partial{}^t\hat{\sigma}_{kl}^{(r)}}{\partial\Delta\omega_{pq}^{(r)}} &= \left(\frac{\partial\mathfrak{R}_{sk}^{(r)}}{\partial\Delta\omega_{pq}^{(r)}} \mathfrak{R}_{il}^{(r)} + \mathfrak{R}_{sk}^{(r)} \frac{\partial\mathfrak{R}_{il}^{(r)}}{\partial\Delta\omega_{pq}^{(r)}} \right) {}^t\sigma_{st}^{(r)} \\ &= (\delta_{ms} \delta_{nk} \mathfrak{R}_{il}^{(r)} + \delta_{mi} \delta_{nl} \mathfrak{R}_{sk}^{(r)}) {}^t\sigma_{st}^{(r)} \frac{\partial\mathfrak{R}_{mn}^{(r)}}{\partial\Delta\omega_{pq}^{(r)}} \end{aligned} \quad (\text{A.4})$$

The rotation $\mathfrak{R}_{mn}^{(r)}$ of phase r is defined in (3.18) as

$$\mathfrak{R}_{mn}^{(r)} = \delta_{mn} + \left(\delta_{mr} - \frac{1}{2} \Delta\omega_{mr}^{(r)} \right)^{-1} \Delta\omega_{rn}^{(r)} \quad (\text{A.5})$$

The derivative of $\mathfrak{R}_{mn}^{(r)}$ is calculated using the chain rule:

$$\frac{\partial\mathfrak{R}_{mn}^{(r)}}{\partial\Delta\lambda^{(m)}} = \frac{\partial\mathfrak{R}_{mn}^{(r)}}{\partial\Delta\omega_{pq}^{(r)}} \frac{\partial\Delta\omega_{pq}^{(r)}}{\partial\Delta\lambda^{(m)}} \quad (\text{A.6})$$

in which

$$\frac{\partial \mathfrak{R}_{mn}^{(r)}}{\partial \Delta \omega_{pq}^{(r)}} = (2\delta_{mp} - \Delta \omega_{mp}^{(r)})^{-1} (\delta_{qn} + \mathfrak{R}_{qn}^{(r)}) \quad (\text{A.7})$$

Consequently, equation (A.4) can be expressed as

$${}_{\sigma} U_{klpq}^{(r)} \equiv \frac{\partial {}^t \hat{\sigma}_{kl}^{(r)}}{\partial \Delta \omega_{pq}^{(r)}} = (\delta_{nk} \mathfrak{R}_{il}^{(r)} {}^t \sigma_{mt}^{(r)} + \delta_{nl} \mathfrak{R}_{sk}^{(r)} {}^t \sigma_{sm}^{(r)}) (2\delta_{mp} - \Delta \omega_{mp}^{(r)})^{-1} (\delta_{qn} + \mathfrak{R}_{qn}^{(r)}) \quad (\text{A.8})$$

Similarly, we have

$${}_{\alpha} U_{klpq}^{(m)} \equiv \frac{\partial {}^t \hat{\alpha}_{kl}^{(m)}}{\partial \Delta \omega_{pq}^{(m)}} = (\delta_{nk} \mathfrak{R}_{il}^{(m)} {}^t \alpha_{mt}^{(m)} + \delta_{nl} \mathfrak{R}_{sk}^{(m)} {}^t \alpha_{sm}^{(m)}) (2\delta_{mp} - \Delta \omega_{mp}^{(m)})^{-1} (\delta_{qn} + \mathfrak{R}_{qn}^{(m)}) \quad (\text{A.9})$$

Taking derivative of (3.30) with respect to $\Delta \lambda^{(m)}$ yields:

$$\frac{\partial \Delta \omega_{pq}^{(m)}}{\partial \Delta \lambda^{(m)}} = \hat{D}_{pqmn}^{(mm)} P_{mnkl} \left((\sigma_{kl}^{(m)} - \alpha_{kl}^{(m)}) + \Delta \lambda^{(m)} \frac{\partial}{\partial \Delta \lambda_m} (\sigma_{kl}^{(m)} - \alpha_{kl}^{(m)}) \right) \quad (\text{A.10})$$

Substituting equations (A.8), (A.9) and (A.10) into (A.3), and then inserting the result into (A.2), gives

$$\frac{\partial}{\partial \Delta \lambda^{(m)}} (\sigma_{ij}^{(m)} - \alpha_{ij}^{(m)}) = C_{ijkl}^{(m)} (\sigma_{kl}^{(m)} - \alpha_{kl}^{(m)}) \quad (\text{A.11})$$

where

$$C_{ijkl}^{(m)} = -(I_{ijmn} + \Delta \lambda^{(m)} W_{ijmn}^{(m)})^{-1} W_{mnkl}^{(m)} \quad (\text{A.12})$$

$$W_{mnkl}^{(m)} = \wp_{mnkl} - (\sigma_{mnst}^{(m)} - \alpha_{mnst}^{(m)}) \hat{D}_{stpq}^{(mm)} P_{pqkl} \quad (\text{A.13})$$

APPENDIX B

LINEARIZATION OF $\Delta\bar{\epsilon}_{ij}$ AND $\Delta\bar{\omega}_{ij}$

We derive the equations for $\Delta\dot{\bar{\epsilon}}_{ij}$ and $\Delta\dot{\bar{\omega}}_{ij}$ consistent with the midpoint integration of rate of deformation and rotation. The left superscript $t + \Delta t$ is omitted.

Taking material time derivative of (3.11) and (3.12) yields:

$$\frac{d}{dt}\Delta\bar{\epsilon}_{ij} = \frac{1}{2} \frac{d}{dt} \left(\frac{\partial\Delta u_i^0}{\partial^{t+\Delta t/2}x_j} + \frac{\partial\Delta u_j^0}{\partial^{t+\Delta t/2}x_i} \right) \quad (\text{B.1})$$

The material time derivative of the first term in the parenthesis of (B.1) can be written as

$$\frac{d}{dt} \left(\frac{\partial\Delta u_i^0}{\partial^{t+\Delta t/2}x_j} \right) = \frac{\partial v_i^0}{\partial^t x_k} \frac{\partial^t x_k}{\partial^{t+\Delta t/2}x_j} + \frac{\partial\Delta u_i^0}{\partial^t x_k} \frac{d}{dt} \left(\frac{\partial^t x_k}{\partial^{t+\Delta t/2}x_j} \right) \quad (\text{B.2})$$

where

$$\frac{d}{dt} \left(\frac{\partial^t x_k}{\partial^{t+\Delta t/2}x_j} \right) = - \frac{\partial^t x_k}{\partial^{t+\Delta t/2}x_m} \frac{d}{dt} \left(\frac{\partial^{t+\Delta t/2}x_m}{\partial^t x_n} \right) \frac{\partial^t x_n}{\partial^{t+\Delta t/2}x_j} \quad (\text{B.3})$$

Consequently, (B.2) can be expressed as

$$\frac{d}{dt} \left(\frac{\partial\Delta u_i^0}{\partial^{t+\Delta t/2}x_j} \right) = \frac{\partial v_i^0}{\partial^{t+\Delta t/2}x_j} - \frac{\partial\Delta u_i^0}{\partial^{t+\Delta t/2}x_m} \frac{d}{dt} \left(\frac{\partial^{t+\Delta t/2}x_m}{\partial^t x_n} \right) \frac{\partial^t x_n}{\partial^{t+\Delta t/2}x_j} \quad (\text{B.4})$$

where

$$\frac{d}{dt} \left(\frac{\partial^{t+\Delta t/2}x_m}{\partial^t x_n} \right) = \frac{\partial}{\partial^t x_n} \left(\frac{d}{dt} \partial^{t+\Delta t/2}x_m \right) = \frac{\partial}{\partial^t x_n} \left\{ \frac{d}{dt} \left(\frac{x_m + {}^t x_m}{2} \right) \right\} = \frac{1}{2} \frac{\partial v_m^0}{\partial^t x_n} \quad (\text{B.5})$$

Substituting (B.5) into (B.4) gives

$$\frac{d}{dt} \left(\frac{\partial \Delta u_i^0}{\partial^{t+\Delta t/2} x_j} \right) = \left(\delta_{im} - \frac{1}{2} \frac{\partial \Delta u_i^0}{\partial^{t+\Delta t/2} x_m} \right) \frac{\partial v_m^0}{\partial^{t+\Delta t/2} x_j} \quad (\text{B.6})$$

Equation (B.6) can be further simplified as

$$\frac{d}{dt} \left(\frac{\partial \Delta u_i^0}{\partial^{t+\Delta t/2} x_j} \right) = \frac{\partial^t x_i}{\partial^{t+\Delta t/2} x_m} \frac{\partial v_m^0}{\partial^{t+\Delta t/2} x_j} \quad (\text{B.7})$$

where the following equality has been utilized.

$$\delta_{im} - \frac{1}{2} \frac{\partial \Delta u_i^0}{\partial^{t+\Delta t/2} x_m} = \frac{\partial}{\partial^{t+\Delta t/2} x_m} \left(\partial^{t+\Delta t/2} x_i - \frac{1}{2} \Delta u_i^0 \right) = \frac{\partial^t x_i}{\partial^{t+\Delta t/2} x_m} \quad (\text{B.8})$$

Defining M_{ijkl} as

$$M_{ijkl} \equiv \frac{\partial^t x_i}{\partial^{t+\Delta t/2} x_k} \frac{\partial x_l}{\partial^{t+\Delta t/2} x_j} \quad (\text{B.9})$$

We have

$$\frac{d}{dt} \left(\frac{\partial \Delta u_i^0}{\partial^{t+\Delta t/2} x_j} \right) = M_{ijkl} v_{k, x_l}^0 \quad (\text{B.10})$$

Substituting (B.10) into (B.1) and performing the same procedure for $\Delta \ddot{\omega}_{ij}$, we obtain the final expressions for $\Delta \dot{\epsilon}_{ij}$ and $\Delta \dot{\omega}_{ij}$ as

$$\Delta \dot{\epsilon}_{ij} = M_{(ij)kl} v_{k, x_l}^0, \quad \Delta \dot{\omega}_{ij} = M_{[ij]kl} v_{k, x_l}^0 \quad (\text{B.11})$$

Note that in the case of backward Euler integration $M_{ijkl} = \delta_{ik} \delta_{jl}$.